NASA TECHNICAL NOTE

NASA TN D-6644
c.1

TECH LIBRARY KAFB, NM
0133175

LOAN COPY: RETUI
AFWL (DOUL)
KIRTLAND AFB, N

NASA TN D-6644

APPLICATION OF A ONE-STRIP INTEGRAL METHOD TO THE UNSTEADY SUPERSONIC AERODYNAMICS OF AN INCLINED FLAT SURFACE

by Robert M. Bennett

Langley Research Center
Hampton, Va. 23365

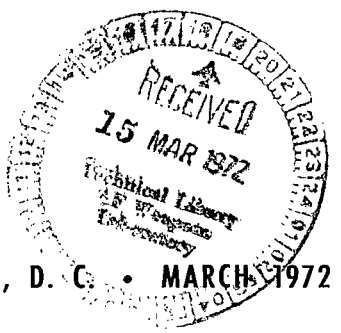

NATIONAL AERONAUTICS AND SPACE ADMINISTRATION • WASHINGTON, D. C. • MARCH 1972

TECH LIBRARY KAFB, NM

0133175

1. Report No. NASA TN D-6644	2. Government Accession No.	3. Recipient's Catalog No.
4. Title and Subtitle APPLICATION OF A ONE-STRIP INTEGRAL METHOD TO THE UNSTEADY SUPERSONIC AERODYNAMICS OF AN INCLINED FLAT SURFACE		5. Report Date March 1972 6. Performing Organization Code
7. Author(s) Robert M. Bennett		8. Performing Organization Report No. L-8047 10. Work Unit No. 136-14-02-02
9. Performing Organization Name and Address NASA Langley Research Center Hampton, Va. 23365		11. Contract or Grant No. 13. Type of Report and Period Covered Technical Note
12. Sponsoring Agency Name and Address National Aeronautics and Space Administration Washington, D.C. 20546		14. Sponsoring Agency Code

15. Supplementary Notes
The material presented herein is based on a thesis entitled "An Analytical Investigation of an Oscillating Wedge in a Supersonic Perfect Gas Flow" submitted in partial fulfillment of the requirements for the degree of Doctor of Philosophy in Aerospace Engineering, North Carolina State University at Raleigh, December 1971.

16. Abstract

The method of integral relations is applied in a one-strip approximation to the perturbation equations governing small motions of an inclined, sharp-edged, flat surface about the mean supersonic steady flow. Algebraic expressions for low-reduced-frequency aerodynamics are obtained and a set of ordinary differential equations are obtained for general oscillatory motion. Results are presented for low-reduced-frequency aerodynamics and for the variation of the unsteady forces with frequency.

The method gives accurate results for the aerodynamic forces at low reduced frequency which are in good agreement with available experimental data. However, for cases in which the aerodynamic forces vary rapidly with frequency, the results are qualitatively correct, but of limited accuracy. Calculations indicate that for a range of inclination angles near shock detachment such that the flow in the shock layer is low supersonic, the aerodynamic forces vary rapidly both with inclination angle and with reduced frequency.

17. Key Words (Suggested by Author(s)) Unsteady aerodynamics Integral method Oscillating wedge	18. Distribution Statement Unclassified – Unlimited		
19. Security Classif. (of this report) Unclassified	20. Security Classif. (of this page) Unclassified	21. No. of Pages 55	22. Price* $3.00

*For sale by the National Technical Information Service, Springfield, Virginia 22151

APPLICATION OF A ONE-STRIP INTEGRAL METHOD TO THE UNSTEADY SUPERSONIC AERODYNAMICS OF AN INCLINED FLAT SURFACE*

By Robert M. Bennett
Langley Research Center

SUMMARY

The method of integral relations is applied in a one-strip approximation to the perturbation equations governing small motions of an inclined, sharp-edged, flat surface about the mean supersonic steady flow. Algebraic expressions for low-reduced-frequency aerodynamics are obtained and a set of ordinary differential equations are obtained for general oscillatory motion. Results are presented for low-reduced-frequency aerodynamics and for the variation of the unsteady forces with frequency.

The method gives accurate results for the aerodynamic forces at low reduced frequency which are in good agreement with available experimental data. However, for cases in which the aerodynamic forces vary rapidly with frequency, the results are qualitatively correct, but of limited accuracy. Calculations indicate that for a range of inclination angles near shock detachment such that the flow in the shock layer is low supersonic, the aerodynamic forces vary rapidly both with inclination angle and with reduced frequency.

INTRODUCTION

Recent developments in flight at high Mach numbers and in computer technology have led to several highly developed methods for the analysis and computation of complex steady flow fields. For example, the finite difference methods (refs. 1 to 3) and the method of integral relations (refs. 4 to 7) have been applied to the analysis of complicated flows over blunt and pointed bodies. However, the surveys of references 8 to 13 indicate that the corresponding unsteady aerodynamics for analyzing flutter, loads, and stability have not been as well developed.

Linearized flow theory was used in much of the early analysis of unsteady supersonic flows (refs. 14 and 15). Recently refined and implemented for an extended range of planforms (ref. 16), linearized theory is still inherently limited to low supersonic Mach numbers and small deflections. The development of piston theory (refs. 17 to 19) permitted extensions to higher Mach numbers, and this theory has been widely applied (refs. 20 and 21, for example). However, piston theory is based on hypersonic small-disturbance theory (ref. 22) and is thus limited to small slopes. It is restricted to values

*The material presented herein is based on a thesis entitled "An Analytical Investigation of an Oscillating Wedge in a Supersonic Perfect Gas Flow" submitted in partial fulfillment of the requirements for the degree of Doctor of Philosophy in Aerospace Engineering, North Carolina State University at Raleigh, December 1971.

of Mach number times deflection angle of less than one, and in the simplified version usually applied, it does not account for the details of the local flow. Other methods used include the simple Newtonian and shock-expansion theories (refs. 23 to 25), but they are also highly simplified and restricted in their range of applicability. Considerable research has been devoted to the refined analytical treatment of the unsteady aerodynamics of flat, sharp-edged surfaces, such as wedges or cones, with simple steady flow fields, in an effort to gain some insight into the limits of the simpler methods and into the effects of strong shock waves and wave interactions on the unsteady flows (refs. 26 to 41). Analysis of the more complex configurations encountered in practice by the methods used for these simpler cases would, however, appear to be prohibitively difficult.

The purpose of this report is to examine the application to unsteady flows of one method that has been used for the computation of steady flow fields – the method of integral relations (refs. 4 to 7) – and to examine some pertinent trends for the unsteady aerodynamic forces.

The method of integral relations is essentially a method for reducing a system of partial differential equations of two (or more) independent variables to an approximating system of ordinary differential equations in one independent variable. Herein, application of the method is made in a one-strip approximation to the unsteady aerodynamics of an inclined, sharp-edged surface such as the compression side of a wedge or flat plate. Both the previously mentioned analytical results and some low-frequency experimental data (ref. 42) for the oscillating wedge are available for comparison. The linearized perturbation equations describing infinitesimal oscillatory motions about the steady flow condition are treated. Linearization and treatment of a specific motion reduces the number of independent variables from three (two space variables plus time) to only the two space variables with frequency as a parameter. The method of integral relations is then applied to further reduce the governing equations to ordinary differential equations in one independent variable. The analysis is outlined and sample results are presented and discussed, with emphasis on the effects of the approach to detachment, surface inclination angle, and ratio of specific heats γ. The oblique-shock perturbation boundary conditions, the calculation of coefficients for a symmetrical wedge from the coefficients for a single surface, and a computer program listing are given as appendixes.

SYMBOLS

a local speed of sound

$B_0 = \sqrt{M_0^2 - 1}$

C chord force

C_p pressure coefficient, $\frac{\overline{p} - \overline{p}_\infty}{\overline{q}_\infty}$

c reference length

D quantity defined by equation (10)

e base of natural system of logarithms, 2.71828

h_x displacement parallel to mean surface position (fig. 1)

h_y plunging displacement normal to mean surface position (fig. 1)

$i = \sqrt{-1}$

k reduced frequency, $\frac{\overline{\omega}\,\overline{c}}{2\overline{V}_\infty}$

$\widetilde{\overline{L}}', \overline{M}'$ motion-related aerodynamic forces and moments measured about the leading edge for a single surface (see eq. (11a) and eq. (11b), respectively)

$\overline{L}_w', \overline{M}_w'$ motion-related aerodynamic forces and moments measured about the leading edge for a symmetrical wedge (see eqs. (B1))

L_j, M_j coefficients in normal-force and moment expressions for a single surface, j = 1,2,3,4,7,8

$L_{j,w}, M_{j,w}$ coefficients in normal-force and moment expressions for a symmetrical wedge, j = 1,2,3,4,7,8

M Mach number, $\frac{V_\infty}{a}$

$P_v = \frac{\partial p_\delta}{\partial v_n}$

$P_\beta = \frac{\partial p_\delta}{\partial \beta_1}$

p pressure

q dynamic pressure

$R_v = \frac{\partial \rho_\delta}{\partial v_n}$

$R_\beta = \frac{\partial \rho_\delta}{\partial \beta_1}$

T shock-layer thickness in y-direction

T_0 shock-layer thickness in y-direction for steady flow

t time

$U_v = \frac{\partial u_\delta}{\partial v_n}$

$U_\beta = \frac{\partial u_\delta}{\partial \beta_1}$

u velocity component in x-direction (fig. 1)

V_∞ free-stream velocity

$V_v = \frac{\partial v_\delta}{\partial v_n}$

$V_\beta = \frac{\partial v_\delta}{\partial \beta_1}$

v velocity component in y-direction (fig. 1)

v_n perturbation of velocity of shock wave measured normal to steady shock wave (fig. 1)

x,y surface coordinates (fig. 1)

x_o,y_o pitch-axis coordinates (as fractions of $\bar{c}$), with x_o measured from leading edge and y_o measured from chord

β_0 shock wave angle for steady flow (fig. 1)

β_1 perturbation of shock wave angle (fig. 1)

γ ratio of specific heats

δ_1 perturbation of shock layer thickness, measured normal to steady shock wave (fig. 1)

δ_w wedge angle $\left(\delta_w = \frac{1}{2}\tan^{-1}\tau \text{ for symmetrical wedge airfoil}\right)$

ϵ perturbation parameter

Θ surface inclination angle

Θ_d surface inclination angle for shock detachment

θ pitch angle

λ_0 included angle between shock and surface for steady flow (fig. 1)

ρ density

τ ratio of airfoil thickness to chord $\bar{c}$

ω circular frequency of oscillation

Subscripts:

h_x, h_y, θ pertaining to perturbation motions of h_x, h_y, or θ, respectively

s denotes complex amplitude of perturbation quantity evaluated at surface

u,l pertaining to upper and lower surface, respectively, for a symmetrical wedge

w pertaining to a symmetrical wedge

δ denotes complex amplitude of perturbation quantity evaluated just aft of shock wave

0 steady flow value in shock layer

1 denotes complex amplitude of perturbation quantity

∞ free-stream value

Superscript:

' pertaining to pitch (or pitching moment) about leading edge

A bar over a symbol indicates a dimensional quantity. A tilde (~) denotes forces normal to the surface.

ANALYSIS

A two-dimensional flat surface with a sharp leading edge and exposed to a supersonic free-stream flow of a perfect gas at a mean inclination angle of Θ is considered while undergoing a specified time-dependent motion (fig. 1). Three types of simple-harmonic oscillations are considered separately – pitching about the leading edge θ, translation normal to the mean position of the surface h_y, and translation parallel to the mean position of the surface h_x. The motion is considered to be an infinitesimal perturbation about the mean or steady-flow condition and leads to a linearized analysis describing the region between the moving surface and shock-wave boundaries beginning at the leading edge and extending a preassigned distance downstream. Linearization of the governing equations permits the application of the boundary conditions at the mean position of the moving boundaries and also permits treatment of any rigid-body, time-dependent motion of the flat surface by superposition of the three motions considered. There are essentially three criteria that govern the amplitude limits for small oscillations: (1) fraction of $\lambda_0 = \beta_0 - \Theta$, (2) fraction of Θ (or for very small Θ, fraction of p_∞), or (3) fraction of $\Theta_d - \Theta$ where Θ_d is the detachment angle. It might be noted that only compression surfaces are treated; however, in a linearized analysis of an expansion surface, the linear theory of reference 14 can be applied by considering the mean surface flow to be the effective free stream. Also for application to wedges, the base pressure is assumed constant and thus does not enter into the motion-related force and moment coefficients.

Development of Perturbation Equations

The governing flow equations written in divergence form for the x,y coordinate system (for example, reference 43, chapter 7) are as follows:

Continuity:

$$\frac{\partial \bar{\rho}}{\partial \bar{t}} + \frac{\partial(\bar{\rho}\bar{u})}{\partial \bar{x}} + \frac{\partial(\bar{\rho}\bar{v})}{\partial \bar{y}} = 0 \tag{1a}$$

x-momentum:

$$\frac{\partial(\bar{\rho}\bar{u})}{\partial \bar{t}} + \frac{\partial\left(\bar{p} + \bar{\rho}\bar{u}^2\right)}{\partial \bar{x}} + \frac{\partial(\bar{\rho}\bar{u}\bar{v})}{\partial \bar{y}} = 0 \tag{1b}$$

y-momentum:

$$\frac{\partial(\bar{\rho}\bar{v})}{\partial \bar{t}} + \frac{\partial(\bar{\rho}\bar{u}\bar{v})}{\partial \bar{x}} + \frac{\partial\left(\bar{p} + \bar{\rho}\bar{v}^2\right)}{\partial \bar{y}} = 0 \tag{1c}$$

Energy:

$$\frac{\partial}{\partial \bar{t}}\left[\frac{\bar{p}}{\gamma} + \frac{(\gamma - 1)}{2\gamma}\bar{\rho}\left(\bar{u}^2 + \bar{v}^2\right)\right] + \frac{\partial}{\partial \bar{x}}\left\{\bar{u}\left[\bar{p} + \frac{(\gamma - 1)}{2\gamma}\bar{\rho}\left(\bar{u}^2 + \bar{v}^2\right)\right]\right\}$$

$$+ \frac{\partial}{\partial \bar{y}}\left\{\bar{v}\left[\bar{p} + \frac{(\gamma - 1)}{2\gamma}\bar{\rho}\left(\bar{u}^2 + \bar{v}^2\right)\right]\right\} = 0 \tag{1d}$$

where the barred quantities are dimensional.

Small variations about the steady flow are considered by substituting in equations (1):

$$\bar{p} = \bar{p}_0 + \epsilon\bar{p}_1(\bar{x},\bar{y})e^{i\bar{\omega}\bar{t}}$$

$$\bar{\rho} = \bar{\rho}_0 + \epsilon\bar{\rho}_1(\bar{x},\bar{y})e^{i\bar{\omega}\bar{t}}$$

$$\bar{u} = \bar{u}_0 + \epsilon\bar{u}_1(\bar{x},\bar{y})e^{i\bar{\omega}\bar{t}}$$

$$\bar{v} = \epsilon\bar{v}_1(\bar{x},\bar{y})e^{i\bar{\omega}\bar{t}}$$

where ϵ is a small quantity; $\bar{\omega}$ is the frequency of oscillation; $\bar{p}_1$, $\bar{\rho}_1$, $\bar{u}_1$, and $\bar{v}_1$ are the complex amplitudes of the perturbations in the flow variables; and $\bar{p}_0$, $\bar{\rho}_0$, and $\bar{u}_0$ pertain to the steady or mean wedge flow. Neglecting terms of order of ϵ^2 and higher gives, for the y-momentum equation, for example,

$$\bar{\rho}_0\bar{u}_0\frac{\partial\bar{v}_1}{\partial\bar{x}} + \frac{\partial\bar{p}_1}{\partial\bar{y}} + i\bar{\omega}\bar{\rho}_0\bar{v}_1 = 0$$

The equations are simpler in form if normalized by the shock-layer variables $\bar{\rho}_0$ and $\bar{u}_0$ and if the shock-layer wavelength $\bar{u}_0/\bar{\omega}$ is used as the characteristic length. By setting $p_1 = \bar{p}_1/\left(\bar{\rho}_0\bar{u}_0^2\right)$, $\rho_1 = \bar{\rho}_1/\bar{\rho}_0$, $u_1 = \bar{u}_1/\bar{u}_0$, $v_1 = \bar{v}_1/\bar{u}_0$, $x = \bar{x}\,\bar{\omega}/\bar{u}_0$, and $y = \bar{y}\,\bar{\omega}/\bar{u}_0$, the following equations result:

y-momentum:

$$\frac{\partial v_1}{\partial x} + \frac{\partial p_1}{\partial y} + iv_1 = 0 \tag{2a}$$

x-momentum:

$$\frac{\partial u_1}{\partial x} + \frac{\partial p_1}{\partial x} + iu_1 = 0 \tag{2b}$$

Energy:

$$\frac{\partial p_1}{\partial x} + \frac{1}{B_0^2}\frac{\partial v_1}{\partial y} + i\,\frac{M_0^2 p_1 - u_1}{B_0^2} = 0 \tag{2c}$$

Continuity:

$$\frac{\partial \rho_1}{\partial x} + \frac{\partial u_1}{\partial x} + \frac{\partial v_1}{\partial y} + i\rho_1 = 0 \tag{2d}$$

where $B_0^2 = M_0^2 - 1$.

Note that the equations have been manipulated to eliminate ρ_1 from equations (2a) to (2c). Equation (2d) is needed only to calculate ρ_1 and will be disregarded here. Thus equations (2a) to (2c) are a system of three simultaneous, linear partial differential equations for p_1, u_1, and v_1 as functions of x and y and with complex, constant coefficients.

Boundary Conditions

Small variations about the steady flow have been considered by substituting in equations (1) for $\bar{p}$, for example,

$$\bar{p} = \bar{p}_0 + \epsilon\bar{p}_1(\bar{x},\bar{y})e^{i\bar{\omega}\bar{t}}$$

where $\bar{p}_1$ is a complex amplitude and ϵ is the real perturbation amplitude parameter θ, h_x, or h_y. The factor $\epsilon e^{i\bar{\omega}\bar{t}}$, common to all terms and thus deleted in equations (2), also appears in all perturbation boundary conditions and is omitted so that the boundary conditions are specified in terms of the complex amplitudes.

Boundary conditions at the leading edge.- For the assumed attached leading-edge shock, the shock-displacement boundary condition is that the shock wave displaces with the leading edge. In terms of the complex perturbation amplitude, this boundary condition for pitching motion is

$$\delta_1(0) = 0 \tag{3a}$$

for plunging motion normal to surface,

$$\delta_1(0) = -\cos \lambda_0 \tag{3b}$$

and for translation parallel to surface,

$$\delta_1(0) = \sin \lambda_0 \tag{3c}$$

Boundary conditions at the surface.- The tangent flow condition at the surface determines the complex amplitude at the surface. For infinitesimal pitching motion, the boundary condition is

$$v_s = -(1 + ix) \tag{4a}$$

for plunging motion normal to the surface,

$$v_s = -i \tag{4b}$$

and for translation parallel to the surface,

$$v_s = 0 \tag{4c}$$

Boundary conditions at the shock wave.- The perturbations of the flow variables just aft of the moving oblique shock wave are discussed in appendix A. The complex amplitudes of the flow variable perturbations are given by equations (A2) in the following form:

$$p_\delta = P_\beta \beta_1 + iP_v \delta_1 \tag{5a}$$

$$u_\delta = U_\beta \beta_1 + iU_v \delta_1 \tag{5b}$$

$$v_\delta = V_\beta \beta_1 + iV_v \delta_1 \tag{5c}$$

where

$$\beta_1 = \frac{d\delta_1}{dx} \cos \lambda_0 \tag{5d}$$

and where $P_\beta = \partial p_\delta / \partial \beta_1$, $U_\beta = \partial u_\delta / \partial \beta_1$, and so forth, are derivatives of the shock relations evaluated at the steady or mean conditions.

Approximate Solution by the Method of Integral Relations

Development of one-strip equations.- For the one-strip integral-relations approach used herein, a linear y-variation of p_1, u_1, and v_1 is assumed. For example,

$$p_1(x,y) = p_s(x) + \left[p_\delta(x) - p_s(x)\right]\frac{y}{T(x)} \tag{6}$$

where subscripts s and δ denote complex perturbation amplitudes evaluated at the surface and just aft of the shock wave, respectively, and $T(x) = T_0 + \frac{\delta_1(x)}{\cos \lambda_0}$ is the total shock-layer thickness. Equation (6) and similar relations for u_1 and v_1 are used in equations (2a) to (2c) and integrated in the y-direction. Products of perturbation quantities are neglected. Sample terms for p_1 are

$$\int_0^T p_1(x,y)dy = \left[p_s(x) + p_\delta(x)\right]\frac{T_0(x)}{2}$$

$$\int_0^T \frac{\partial p_1(x,y)}{\partial y}\,dy = p_\delta(x) - p_s(x)$$

and, with the use of Leibniz' rule,

$$\int_0^T \frac{\partial p_1(x,y)}{\partial x}\,dy = \frac{d}{dx}\int_0^T p_1(x,y)dy - \frac{dT}{dx}\,p_\delta(x)$$

$$= \left[\frac{dp_s(x)}{dx} + \frac{dp_\delta(x)}{dx}\right]\frac{T_0(x)}{2} + \frac{1}{2}\left[p_s(x) - p_\delta(x)\right]\frac{dT_0(x)}{dx}$$

The results of this procedure are as follows:

$$\frac{d}{dx}(p_\delta + p_s + u_\delta + u_s) - \frac{1}{T_0}(p_\delta - p_s + u_\delta - u_s)\frac{dT_0}{dx} + i(u_\delta + u_s) = 0$$

$$\frac{d}{dx}(v_\delta + v_s) - \frac{1}{T_0}(v_\delta - v_s)\frac{dT_0}{dx} + \frac{2}{T_0}(p_\delta - p_s) + i(v_\delta + v_s) = 0$$

$$\frac{d}{dx}(p_\delta + p_s) - \frac{1}{T_0}(p_\delta - p_s)\frac{dT_0}{dx} + \frac{2}{T_0 B_0{}^2}(v_\delta - v_s)$$

$$+ \frac{i}{B_0{}^2}\left[M_0{}^2(p_\delta + p_s) - (u_\delta + u_s)\right] = 0$$

Now,

$$T_0(x) = x \tan \lambda_0$$

and

$$\frac{dT_0(x)}{dx} = \tan \lambda_0$$

Furthermore, the terms subscripted by δ are given by the boundary conditions just aft of the shock wave (eqs. (5a) to (5c)). For example,

$$p_\delta(x) = P_\beta \beta_1(x) + iP_v \delta_1(x)$$

and thus

$$\frac{dp_\delta}{dx} = P_\beta \frac{d\beta_1(x)}{dx} + iP_v \frac{d\delta_1(x)}{dx} = P_\beta \frac{d\beta_1(x)}{dx} + i \frac{P_v}{\cos \lambda_0} \beta_1(x)$$

as $\beta_1 = \frac{d\delta_1}{dx} \cos \lambda_0$ (eq. (5d)). Developing and using similar expressions for du_δ/dx and dv_δ/dx gives the following equations:

$$x \frac{d\beta_1}{dx} + \left[\frac{2P_\beta}{V_\beta} \cot \lambda_0 - 1 + ix\left(1 + \frac{V_v}{V_\beta \cos \lambda_0}\right)\right]\beta_1$$

$$+ i\left[\frac{2P_v}{V_\beta} \cot \lambda_0 - (1 - ix) \frac{V_v}{V_\beta}\right]\delta_1 - \frac{2 \cot \lambda_0}{V_\beta} p_s$$

$$= - \frac{x}{V_\beta} \frac{dv_s}{dx} - \frac{v_s}{V_\beta}(1 + ix) \tag{7a}$$

$$x \frac{du_s}{dx} + (1 + ix)u_s + x \frac{dp_s}{dx} + p_s + x(P_\beta + U_\beta)\frac{d\beta_1}{dx}$$

$$- \left[P_\beta + (1 - ix)U_\beta - ix \frac{P_v + U_v}{\cos \lambda_0}\right]\beta_1 - i\left[P_v + U_v(1 - ix)\right]\delta_1 = 0 \tag{7b}$$

$$x\frac{dp_s}{dx} + \left(1 + ix\frac{M_0^2}{B_0^2}\right)p_s - i\frac{x}{B_0^2}u_s + xP_\beta\frac{d\beta_1}{dx}$$

$$+ \left[\frac{2V_\beta}{B_0^2\tan\lambda_0} - P_\beta\left(1 - ix\frac{M_0^2}{B_0^2}\right) + ix\left(\frac{P_v}{\cos\lambda_0} - \frac{U_\beta}{B_0^2}\right)\right]\beta_1$$

$$+ i\left[\frac{2V_v}{B_0^2\tan\lambda_0} - P_v\left(1 - ix\frac{M_0^2}{B_0^2}\right) - ix\frac{U_v}{B_0^2}\right]\delta_1 = \frac{2v_s}{B_0^2\tan\lambda_0} \tag{7c}$$

$$\frac{d\delta_1}{dx} = \frac{\beta_1}{\cos\lambda_0} \tag{7d}$$

The partial differential equations (eqs. (2)) and their boundary conditions have been transformed to four inhomogeneous, complex, variable-coefficient, ordinary differential equations in p_s, u_s, δ_1, and β_1. The known surface velocity $v_s(x)$ appears as a forcing function, and the required initial conditions are also contained in equations (7) as will be subsequently shown.

Initial values at the leading edge.- Taking the limit as $x \to 0$ in equations (7) gives

$$\beta_1(0) = \frac{v_s(0)}{V_\beta} - i\frac{V_v}{V_\beta}\delta_1(0) \tag{8a}$$

$$p_s(0) = P_\beta\beta_1(0) + iP_v\delta_1(0) \tag{8b}$$

$$u_s(0) = U_\beta\beta_1(0) + iU_v\delta_1(0) \tag{8c}$$

These conditions are the exact quasi-static linearized conditions from oblique-shock theory.

Initial derivatives at the leading edge.- Differentiating equations (7) with respect to x, taking the limit as $x \to 0$, and applying equations (8) gives an algebraic system which can be solved for $\left.\frac{d\beta_1}{dx}\right|_{x=0}$, $\left.\frac{dp_s}{dx}\right|_{x=0}$, and $\left.\frac{du_s}{dx}\right|_{x=0}$

The results are as follows:

$$\left.\frac{d\beta_1}{dx}\right|_{x=0} = \frac{1}{D}\left\{\left(1 - B_0{}^2\tan^2\lambda_0\right)\left.\frac{dv_s}{dx}\right|_{x=0} - i\tan\lambda_0\left[\frac{B_0{}^2\tan\lambda_0}{2}v_s(0)\right.\right.$$

$$+ i\left(M_0{}^2P_v - U_v + V_v\frac{B_0{}^2}{2}\tan\lambda_0\right)\delta_1(0) + \left(M_0{}^2P_\beta - U_\beta + \frac{V_v}{\sin\lambda_0}\right.$$

$$\left.\left.\left.+ \frac{B_0{}^2}{2}V_\beta\tan\lambda_0 + \frac{P_vB_0{}^2}{\cos\lambda_0}\right)\beta_1(0)\right]\right\} \tag{9a}$$

$$\left.\frac{dp_s}{dx}\right|_{x=0} = P_\beta\left.\frac{d\beta_1}{dx}\right|_{x=0} + \tan\lambda_0\left.\frac{dv_s}{dx}\right|_{x=0} + i\frac{\tan\lambda_0}{2}\left[v_s(0) + iV_v\delta_1(0)\right.$$

$$\left.+ \left(V_\beta + \frac{2P_v}{\sin\lambda_0}\right)\beta_1(0)\right] \tag{9b}$$

and

$$\left.\frac{du_s}{dx}\right|_{x=0} = -\left.\frac{dp_s}{dx}\right|_{x=0} - iu_s(0) \tag{9c}$$

In equation 9(a),

$$D = V_\beta + P_\beta B_0{}^2\tan\lambda_0 \tag{10}$$

Definition of force and moment coefficients.- The motion-related aerodynamic force and moment coefficients are defined for a single (upper; see fig. 1) surface by

$$\tilde{\bar{L}}' = -\int_0^{\bar{c}}\left[\bar{p}(\bar{x}) - \bar{p}_0\right]d\bar{x} = 4\bar{q}_\infty\bar{c}k^2\left[2\left(\tilde{L}_1 + i\tilde{L}_2\right)\frac{\bar{h}_y}{\bar{c}}\right.$$

$$\left.+ \left(\tilde{L}_3' + i\tilde{L}_4'\right)\theta + 2\left(\tilde{L}_7 + i\tilde{L}_8\right)\frac{\bar{h}_x}{\bar{c}}\right]e^{i\bar{\omega}\bar{t}} \tag{11a}$$

$$\overline{M}' = \int_0^{\overline{c}} \overline{x}\left[\overline{p}(\overline{x}) - \overline{p}_0\right]d\overline{x} = -2\overline{q}_\infty \overline{c}^2 k^2 \left[2\left(M_1' + iM_2'\right)\frac{\overline{h}_y}{\overline{c}}\right.$$

$$\left. + \left(M_3' + iM_4'\right)\theta + 2\left(M_7' + iM_8'\right)\frac{\overline{h}_x}{\overline{c}}\right]e^{i\overline{\omega}\overline{t}} \tag{11b}$$

In equations (11), moments and displacements are measured at the leading edge. These definitions are similar to those often used in two-dimensional supersonic flutter analysis (e.g., ref. 14). Here, however, the force is normal to the surface (indicated by ~ over the L), rather than in the lift direction, and subscripts 7 and 8 pertain to fore and aft translation parallel to the mean surface position. (The symbol N and the subscripts 5 and 6 are often used for unsteady flap hinge moments and for pertaining to a flap, respectively; see ref. 14.) It might also be noted that no forces along the surface are generated, since the effects of viscous skin friction have been neglected and the base pressure has been assumed to remain constant. In appendix B the aerodynamic coefficients for a wedge are given in terms of these definitions (eqs. (11)).

Low-k solution based on initial conditions.- The independent variable x $\left(\text{that is, } \overline{x}\,\overline{\omega}/\overline{u}_0\right)$ serves as a nondimensional length scale for the oscillating wedge. For a specific value of $\overline{x}$ (such as $\overline{c}$ or unity), $k = \left(\overline{u}_0/2\overline{V}_\infty\right)x$ and thus small values of x imply small values of k. The surface pressure for small values of x (and hence k) can be approximated as

$$p_s(x) = p_s(0) + \left.\frac{dp_s}{dx}\right|_{x=0} x \tag{12}$$

Using the boundary conditions given by equations (3) in equations (8) and (9) and integrating for the force and moment coefficients as defined by equations (11) gives for small values of k and for a single exposed surface

$$\left.\begin{aligned} \tilde{L}_1 = \frac{3}{4}M_1' &= -\frac{\overline{\rho}_0}{2\overline{\rho}_\infty}\left.\frac{dp_{s,h_y}}{dx}\right|_{x=0} \\ k\tilde{L}_2 = kM_2' &= -\frac{\overline{\rho}_0\overline{u}_0}{2\overline{\rho}_\infty\overline{u}_\infty}p_{s,h_y}(0) \\ k^2\tilde{L}_3' = k^2M_3' &= -\frac{\overline{\rho}_0\overline{u}_0^2}{2\overline{\rho}_\infty\overline{u}_\infty^2}p_{s,\theta}(0) \end{aligned}\right\} \tag{13}$$

(Equations continued on next page)

$$
\left.
\begin{aligned}
k\tilde{L}_4' &= \frac{3}{4}\,kM_4' = -\frac{\overline{\rho}_0\overline{u}_0}{2\overline{\rho}_\infty\overline{u}_\infty}\left.\frac{dp_{s,\theta}}{dx}\right|_{x=0} \\
\tilde{L}_7 &= \frac{3}{4}\,M_7' = -\frac{\overline{\rho}_0}{2\overline{\rho}_\infty}\left.\frac{dp_{s,h_x}}{dx}\right|_{x=0} \\
k\tilde{L}_8 &= kM_8' = -\frac{\overline{\rho}_0\overline{u}_0}{2\overline{\rho}_\infty\overline{u}_\infty}\,p_{s,h_x}(0)
\end{aligned}
\right\}
$$

Evaluating equations (13) using equations (3), (4), (8), and (9) leads to the following algebraic expressions for the coefficients involving only the properties of the steady flow $\overline{p}_0$, $\overline{u}_0$, and so forth, and the shock-wave derivatives P_β, V_v, and so forth:

$$
\left.
\begin{aligned}
k\tilde{L}_2 &= \frac{\overline{\rho}_0\overline{u}_0}{2\overline{\rho}_\infty\overline{u}_\infty V_\beta}\left(P_\beta - A_1\cos\lambda_0\right) \\
k^2\tilde{L}_3' &= \frac{\overline{\rho}_0\overline{u}_0{}^2}{2\overline{\rho}_\infty\overline{u}_\infty{}^2 V_\beta}\,P_\beta \\
k\tilde{L}_8 &= \frac{\overline{\rho}_0\overline{u}_0}{2\overline{\rho}_\infty\overline{u}_\infty V_\beta}\,A_1\sin\lambda_0 \\
\tilde{L}_7 &= \frac{\overline{\rho}_0\tan\lambda_0}{2\overline{\rho}_\infty V_\beta D}\left[\left(V_v + M_0{}^2P_\beta\sin\lambda_0\right)A_1 - P_\beta A_2\sin\lambda_0\right] \\
\tilde{L}_1 &= -\cot\lambda_0\tilde{L}_7 - \frac{\overline{\rho}_0 A_3}{2\overline{\rho}_\infty} \\
k\tilde{L}_4' &= \frac{\overline{\rho}_0\overline{u}_0}{2\overline{\rho}_\infty\overline{u}_\infty}\left[\tan\lambda_0 + \frac{P_\beta\left(1 - B_0{}^2\tan^2\lambda_0\right)}{D} + A_3\right]
\end{aligned}
\right\} \qquad (14)
$$

where

$$A_1 = P_\beta V_v - P_v V_\beta$$

$$A_2 = U_\beta V_v - U_v V_\beta$$

$$A_3 = \tan \lambda_0 \left\{ 1 - \frac{1}{V_\beta D} \left[\frac{A_1}{\sin \lambda_0} - P_\beta \left(U_\beta - M_0^2 P_\beta - V_\beta B_0^2 \tan \lambda_0 \right) \right] \right\}$$

and D is given by equation (10).

Numerical solution of one-strip equations.- To determine the variation of the force and moment coefficients with k, equations (7) are numerically integrated by using a computer subroutine for first-order, real, ordinary differential equations. These complex equations (eqs. (7)) are converted to a system of eight coupled, first-order equations relating the real (Re) and imaginary (Im) parts of δ_1, β_1, u_s, and p_s. Initial values and derivatives at a small value of x are calculated from equation (12), for example, which requires using equations (8) and (9) for starting the numerical integration of the differential equations. As $k = \frac{\bar{\omega}\bar{c}}{2\bar{V}_\infty} = \frac{\bar{u}_0 x}{2\bar{V}_\infty}$, running integrals over x of the real and imaginary parts of the pressure give the variation of the aerodynamic coefficients with k. By using the definitions given as equations (11), the coefficients are related to the integral of the pressure for a single exposed surface as follows:

$$\tilde{L}_1 = -\frac{\bar{\rho}_0}{\bar{\rho}_\infty x^2} \int_0^x \mathrm{Re}\left[p_{h_y}(\xi) \right] d\xi$$

$$\tilde{L}_7 = -\frac{\bar{\rho}_0}{\bar{\rho}_\infty x^2} \int_0^x \mathrm{Re}\left[p_{h_x}(\xi) \right] d\xi$$

$$k\tilde{L}_2 = -\frac{\bar{\rho}_0 \bar{u}_0}{2\bar{\rho}_\infty \bar{u}_\infty x} \int_0^x \mathrm{Im}\left[p_{h_y}(\xi) \right] d\xi$$

$$k\tilde{L}_8 = -\frac{\bar{\rho}_0 \bar{u}_0}{2\bar{\rho}_\infty \bar{u}_\infty x} \int_0^x \mathrm{Im}\left[p_{h_x}(\xi) \right] d\xi$$

$$M_1' = -\frac{2\bar{\rho}_0}{\bar{\rho}_\infty x^3} \int_0^x \mathrm{Re}\left[p_{h_y}(\xi) \right] \xi \, d\xi$$

$$M_7' = -\frac{2\bar{\rho}_0}{\bar{\rho}_\infty x^3} \int_0^x \mathrm{Re}\left[p_{h_x}(\xi) \right] \xi \, d\xi$$

$$kM_2' = -\frac{\bar{\rho}_0\bar{u}_0}{\bar{\rho}_\infty\bar{u}_\infty x^2}\int_0^x \mathrm{Im}\left[p_{h_y}(\xi)\right]\xi\, d\xi$$

$$kM_8' = -\frac{\bar{\rho}_0\bar{u}_0}{\bar{\rho}_\infty\bar{u}_\infty x^2}\int_0^x \mathrm{Im}\left[p_{h_x}(\xi)\right]\xi\, d\xi$$

where ξ is the variable of integration in the x-direction. Similarly, for pitch,

$$k^2\tilde{L}_3' = -\frac{\bar{\rho}_0\bar{u}_0^2}{2\bar{\rho}_\infty\bar{u}_\infty 2x}\int_0^x \mathrm{Re}\left[p_\theta(\xi)\right]d\xi$$

$$k\tilde{L}_4' = -\frac{\bar{\rho}_0\bar{u}_0}{\bar{\rho}_\infty\bar{u}_\infty x^2}\int_0^x \mathrm{Im}\left[p_\theta(\xi)\right]d\xi$$

$$k^2M_3' = -\frac{\bar{\rho}_0\bar{u}_0^2}{\bar{\rho}_\infty\bar{u}_\infty 2x^2}\int_0^x \mathrm{Re}\left[p_\theta(\xi)\right]\xi\, d\xi$$

$$kM_4' = -\frac{2\bar{\rho}_0\bar{u}_0}{\bar{\rho}_\infty\bar{u}_\infty x^3}\int_0^x \mathrm{Im}\left[p_\theta(\xi)\right]\xi\, d\xi$$

A computing program is given in appendix C which calculates twice the above integrals. The trapezoidal rule is used for numerical integration of the surface pressures in the integrals to determine the coefficients.

RESULTS AND DISCUSSION

Comments on the Method

One result of applying the method of integral relations is a change in the region of influence of the governing differential equations. Disturbances propagate along the normal coordinate rather than along characteristics and the description of wave-type phenomena is thus altered. The application to steady supersonic flow over pointed bodies has been discussed in reference 7. It was found that although the results of the method differed in detail, the exact wave behavior was approximated as a result of compensating effects.

The integral method has also been applied to the perturbation of plane entropy layers which involves extensive wave effects with favorable results (ref. 6). As discussed in references 29 and 37, the acoustic waves generated by the surface and shock wave are important factors in determining the unsteady forces on the wedge. The description of these wave phenomena by the one-strip integral method (eqs. (7)) is investigated by applying the method to a steady angular perturbation of a wedge surface. The results are compared in figure 2 with the exact solution from hypersonic small-disturbance theory of reference 29. The results of the one-strip method do not follow the exact wave pattern, but approximate it in a smoothed oscillatory fashion. This is thus an important limitation of the method if local details are important. However, it might also be noted that the example cited contains a slope discontinuity. For cases with continuous slopes, this smoothing should be less severe.

Low-Reduced-Frequency Aerodynamic Forces

Comparisons with other analytical results and experiment.- The exact solutions for the low-frequency or stability-derivative-type aerodynamics of references 27 and 36 are available for a symmetrical wedge pitching about an axis located on the chord at any chordwise location. Direct algebraic comparisons with these results would be rather lengthy. The equations of reference 27 were programed and calculations made for an extensive range of M, γ, and Θ. The results obtained were identical to the results from using equations (14) and the transformation equations of appendix B. Furthermore, the results presented in the figures of reference 36 were also reproduced by using the one-strip equations. However, no results for $\tilde{L}_1$ are available for comparison. Although not rigorously demonstrated, the results of the one-strip approximation (eqs. (14)) are thought to be exact for the low-frequency aerodynamics. Further comparisons with the linear theory of reference 14 and the second-order theory of reference 44 were also made by expanding the one-strip results in powers of Θ and obtaining identical results. Similar expansions for hypersonic small-disturbance conditions agreed with the results of reference 29.

With the previously noted smoothing of the wave behavior by the method of integral relations, the degree of validity of the present results may seem surprising. It was found in reference 36, however, that linear functions in x and y satisfied the perturbation equations for the pitching wedge and the caret wing. The linear y-function is the form of solution assumed by the one-strip method of integral relations (eq. (6)) and the linear x-function is the form assumed for the low-frequency approximation (eq. (12)).

Results calculated by using equations (14) are compared with the experimental data for a symmetrical pitching wedge (ref. 42) in figures 3 and 4. Generally good agreement is obtained, with the best agreement being for the thinner wedge and higher Mach number.

Selected analytical results.- The six normal-force coefficients (eqs. (13) and (14)) for a single inclined surface are presented in figures 5 and 6 for $M = 2$ and $M = \infty$, respectively, and for several values of the ratio of specific heats γ. All coefficients vary considerably with inclination angle, particularly for $M = \infty$, and approach infinity as detachment is approached. The coefficients $\tilde{L}_1$ and $k\tilde{L}_4'$ also change sign as detachment is approached. As the damping-in-pitch (about the leading edge) is related to $k\tilde{L}_4'$ (e.g., see eqs. (13)), the damping-in-pitch thus changes to an unstable value near detachment. This unstable pitch-damping has also been discussed in reference 36.

The effect of γ (figs. 5 and 6) is primarily to shift the detachment angle, and thus even small changes in the value of γ have large effects near detachment.

The fore and aft coefficients $\tilde{L}_7$ and $k\tilde{L}_8$ are, of course, zero for $\Theta = 0$ and are somewhat small until the detachment angle is approached.

It appears that the detachment condition leads to singular behavior in each stability derivative. That such is the case for the static forces is apparent from the charts of reference 45 which show that $dp_s/d\Theta$ is infinite at detachment. For sonic local embedded flow the static derivatives are not infinite, but are extremely large. Furthermore, as discussed in reference 46, the quantity D (see eq. (10)) in the denominator of the dynamic derivatives (see eqs. (14)) vanishes at the Crocco point, which occurs for a value of Θ slightly larger than for sonic local flow and less than Θ_d. For the small range of Θ for subsonic but attached flow, theories for an infinite wedge are no longer valid, as the subsonic flow field between the shock and the surface is not uniform for a finite wedge (ref. 47). Some implications of the approach to detachment on the flutter characteristics of diamond airfoils have been discussed in reference 25.

Generally, in linear aerodynamics, the presence of a singularity such as that shown herein indicates a need for a more complete treatment of the nonlinear governing flow equations in order to describe a more realistic behavior. In the present paper, however, at least up to conditions of sonic local flow, accurate infinitesimal amplitude results are obtained. Furthermore, the usual transonic refinement to linear theory retains a local x-derivative of the steady flow field as a variable coefficient in the unsteady equations (ref. 48); herein, the term is zero. The present results suggest that infinitesimal motion has limited practical significance near detachment since even small finite amplitudes result in rapidly varying aerodynamic forces. Near detachment, the condition for infinitesimal motion is that the amplitude of motion must be small compared with $\Theta_d - \Theta$, where Θ_d is the detachment angle.

Variation of Aerodynamic Forces With Reduced Frequency

Comparisons with other results.- There are no results known to the author for the variation of the aerodynamic forces with reduced frequency as computed from the super-

sonic flow solution for the wedge of reference 26 or the extension of reference 27. Furthermore, such computations would be a rather lengthy task. Consequently, typical results of the integration of equations (7) are compared for $\Theta = 0$ with supersonic linear theory for the flat plate (ref. 14), are compared for small Θ with second-order theory (ref. 44), and are compared with hypersonic small-disturbance theory (refs. 29 and 30) in figures 7 to 9. In general, the one-strip integral method predicts the correct trends, but is accurate only when the frequency effects are small such as for thin surfaces at high Mach numbers (fig. 9). Such a result might be anticipated in view of the previously discussed treatment of wave behavior by the integral method.

Selected results.- The results of integrating equations (7) for $M = \infty$, $\gamma = 7/5$, and $\Theta = 25^{\circ}$ are given in figure 10. The frequency effects are small for $k < 1$; essentially no frequency effects are apparent for the usual range of interest for hypersonic speeds of $k < 0.1$.

As previously discussed, the low-frequency aerodynamic coefficients vary rapidly with inclination angle as detachment is approached. Corresponding frequency effects are presented in figure 11. A very strong frequency dependence even at low reduced frequencies is evident as detachment is approached. In view of the previous comparisons with other theories (figs. 7 to 9), these results may be considered only qualitative in nature. The trends indicated are important ones, however. For example, the coefficient $k\tilde{L}_4'$ for $\Theta = 22^{\circ}$ (fig. 11) varies so rapidly as to suggest that the linear results may be physically unrealistic. If a nonlinear analysis were carried out for this region, then the phenomena of subharmonics or higher harmonics may occur which are rejected by the linear theory. In fact, the quasi-static results of references 34 and 39 indicate that for some conditions the unsteady pressure waveform is not a single harmonic of the frequency of oscillation and that shifts in the mean pressure level can occur even for moderate amplitudes of motion. Taking such nonlinear phenomena into account in a full dynamic analysis would require considerably more effort than would be required for a conventional linear analysis.

Rapid variation of the coefficients with k may cause rapid variation of flutter characteristics with parameters that strongly influence the resulting k at flutter (such as the mass ratio; e.g., see ref. 49).

CONCLUDING REMARKS

A one-strip approximation of the method of integral relations has been applied to the perturbation equations describing small motions of an inclined flat surface. Accurate results were obtained with the method for the aerodynamic forces at low reduced frequency. Good agreement with available experimental data for a pitching wedge was also

obtained. The method, in the one-strip approximation at least, is of limited accuracy for cases in which the aerodynamic forces vary rapidly with reduced frequency.

The results indicate that for the range of inclination angles near shock detachment, the aerodynamic forces vary rapidly both with inclination angle and with reduced frequency.

Langley Research Center,
National Aeronautics and Space Administration,
Hampton, Va., January 26, 1972.

APPENDIX A

PERTURBATIONS OF FLOW VARIABLES AT A MOVING OBLIQUE SHOCK WAVE

The incremental values p_1, ρ_1, u_1, and v_1 resulting from perturbations of slope and normal velocity of the moving oblique shock wave are required as boundary conditions for a perturbation analysis. The shock-wave perturbation is measured normal to the steady shock wave, as shown in figure 1. The appropriate perturbations of the Rankine-Hugoniot conditions in a coordinate system alined with the steady shock wave have been developed in reference 26. They have also been given in the surface coordinate system used here (fig. 1) specialized to $\gamma = 7/5$ (refs. 26 and 27), and for general values of γ but in somewhat different nondimensional units (refs. 26 and 36). Here, the shock derivatives are given for general γ in the nondimensional units used for equations (2) and are presented in much simpler algebraic form than those of references 26, 27, and 36.

With the complex amplitude of the normal velocity of the shock wave given by

$$v_n = i\delta_1(x) \tag{A1}$$

the complex amplitudes of the perturbations of the flow variables are written in the following form:

$$\left.\begin{aligned} p_\delta &= P_\beta\beta_1 + iP_v\delta_1 \\ \rho_\delta &= R_\beta\beta_1 + iR_v\delta_1 \\ u_\delta &= U_\beta\beta_1 + iU_v\delta_1 \\ v_\delta &= V_\beta\beta_1 + iV_v\delta_1 \end{aligned}\right\} \tag{A2}$$

where $P_\beta = \partial p_\delta/\partial\beta_1$, $P_v = \partial p_\delta/\partial v_n$, and so forth, are evaluated at the steady shock wave position and subscript δ denotes perturbation of conditions just aft of the shock wave. By letting

$$\left.\begin{aligned} M_n &= M_\infty \sin\beta_0 \\ U_n &= \frac{2(M_n^2 + 1)}{(\gamma + 1)M_n^2} \end{aligned}\right\} \tag{A3}$$

the shock derivatives can be written as

$$\left.\begin{aligned} P_v &= \frac{4\bar{\rho}_\infty \bar{u}_\infty}{(\gamma+1)\bar{\rho}_0 \bar{u}_0} \sin\beta_0 \\ R_v &= \frac{4\bar{\rho}_0}{(\gamma+1)\bar{\rho}_\infty M_n^2 \sin\beta_0} \\ U_v &= -U_n \sin\lambda_0 \\ V_v &= U_n \cos\lambda_0 \end{aligned}\right\} \tag{A4}$$

and

$$\left.\begin{aligned} P_\beta &= \frac{\bar{V}_\infty P_v}{\bar{u}_0} \cos\beta_0 \\ R_\beta &= R_v \cos\beta_0 \\ U_\beta &= \frac{\bar{V}_\infty U_n}{\bar{u}_0} \sin\Theta - \frac{\bar{\rho}_0}{\bar{\rho}_\infty} P_v \cos\lambda_0 \\ V_\beta &= \frac{\bar{V}_\infty U_n}{\bar{u}_0} \cos\Theta - \frac{\bar{\rho}_0}{\bar{\rho}_\infty} P_v \sin\lambda_0 \end{aligned}\right\} \tag{A5}$$

These relations (eqs. (A4) and (A5)) reduce to those given in references 29 and 30 in the hypersonic small-disturbance limit. It can also be shown with a similar development that perturbations of the shock wave tangential to the steady shock position result in second-order perturbations in the flow variables.

The steady-flow values of pressure, density, and velocities within the shock layer are given in reference 45 as functions of γ, M_∞, and β_0. The corresponding relation between β_0 and Θ is also given as a cubic in $\sin^2\beta_0$ with coefficients as functions of γ and Θ. These relations are solved numerically for the steady-flow-field parameters.

APPENDIX B

CALCULATION OF AERODYNAMIC COEFFICIENTS FOR A WEDGE FROM SURFACE COEFFICIENTS

General Comments

The unsteady aerodynamic coefficients for a single isolated surface have been derived in this report for rigid-body pitch and translation perpendicular and parallel to the surface. The coefficients and k were based on the length of the surface $\bar{c}$, and the pitch axis was located at the leading edge. The coefficients for a symmetrical wedge at an angle of attack are given in this appendix in terms of the surface coefficients. The pitch axis is assumed to be on the wedge midplane or chord. The derivation of these relations is briefly outlined and the results are summarized.

Force and Motion Transfer

The forces and moments for a symmetrical wedge (subscript w) are related to the previously given forces and moments for a single surface by

$$\left.\begin{aligned} \bar{L}'_w &= \pm\tilde{\bar{L}}' \cos \delta_w \\ \bar{C}_w &= -\tilde{\bar{L}}' \sin \delta_w \\ \bar{M}'_w &= \pm\bar{M}' \end{aligned}\right\} \tag{B1}$$

where the upper sign is for an upper surface. The pitch axis is displaced from the surface and the chords are related by

$$\left.\begin{aligned} \bar{c} &= \frac{\bar{c}_w}{\cos \delta_w} \\ \bar{x}_o &= \bar{x}_{o,w} \cos \delta_w \\ \bar{y}_o &= -\bar{x}_{o,w} \sin \delta_w \end{aligned}\right\} \tag{B2}$$

The perturbation displacements are related by

$$\left.\begin{aligned} \bar{h}_y &= \pm\bar{h}_{y,w}\cos\delta_w - \bar{h}_{x,w}\sin\delta_w - \bar{x}_{o,w}(\cos\delta_w)\theta \\ \bar{h}_x &= \bar{h}_{x,w}\cos\delta_w \pm \bar{h}_{y,w}\sin\delta_w - \bar{x}_{o,w}(\sin\delta_w)\theta \\ \theta_u &= \theta; \quad \theta_l = -\theta \end{aligned}\right\} \tag{B3}$$

where again the upper sign pertains to the upper surface.

The force and moment coefficients are defined by equations (11) for a single surface. By defining the coefficients for the wedge in a manner similar to equations (11), the coefficients for the surface and the wedge can be related through the use of equations (B1) for the dimensional forces. Then substituting equations (B2) and (B3) into the expression for the surface coefficients, the wedge coefficients can be equated to the corresponding combination of surface coefficients.

Coefficients for Wedge

The results for the coefficients of lift and moment for the wedge are

$$\left.\begin{aligned} L_{1,w} &= \left(\tilde{L}_{1,u} + \tilde{L}_{1,l}\right) + \left(\tilde{L}_{7,u} + \tilde{L}_{7,l}\right)\tan\delta_w \\ L_{2,w} &= \left(\tilde{L}_{2,u} + \tilde{L}_{2,l}\right) + \left(\tilde{L}_{8,u} + \tilde{L}_{8,l}\right)\tan\delta_w \\ L'_{3,w} &= \left(\tilde{L}'_{3,u} + \tilde{L}'_{3,l}\right)\Big/\cos^2\delta_w \\ L'_{4,w} &= \left(\tilde{L}'_{4,u} + \tilde{L}'_{4,l}\right)\Big/\cos^2\delta_w \\ L_{7,w} &= \left(\tilde{L}_{7,u} - \tilde{L}_{7,l}\right) - \left(\tilde{L}_{1,u} - \tilde{L}_{1,l}\right)\tan\delta_w \\ L_{8,w} &= \left(\tilde{L}_{8,u} - \tilde{L}_{8,l}\right) - \left(\tilde{L}_{2,u} - \tilde{L}_{2,l}\right)\tan\delta_w \end{aligned}\right\} \tag{B4}$$

and

$$\left.\begin{aligned}
M'_{1,w} &= \left[\left(M'_{1,u} + M'_{1,l}\right) + \left(M'_{7,u} + M'_{7,l}\right)\tan\delta_w\right]\Big/\cos^2\delta_w \\
M'_{2,w} &= \left[\left(M'_{2,u} + M'_{2,l}\right) + \left(M'_{8,u} + M'_{8,l}\right)\tan\delta_w\right]\Big/\cos^2\delta_w \\
M'_{3,w} &= \left(M'_{3,u} + M'_{3,l}\right)\Big/\cos^4\delta_w \\
M'_{4,w} &= \left(M'_{4,u} + M'_{4,l}\right)\Big/\cos^4\delta_w \\
M'_{7,w} &= \left[\left(M'_{7,u} - M'_{7,l}\right) - \left(M'_{1,u} - M'_{1,l}\right)\tan\delta_w\right]\Big/\cos^2\delta_w \\
M'_{8,w} &= \left[\left(M'_{8,u} - M'_{8,l}\right) - \left(M'_{2,u} - M'_{2,l}\right)\tan\delta_w\right]\Big/\cos^2\delta_w
\end{aligned}\right\} \qquad \text{(B5)}$$

The relationship for reduced frequency for the wedge is

$$\left.\begin{aligned}
k &= k_u \cos\delta_w \\
k &= k_l \cos\delta_w
\end{aligned}\right\} \qquad \text{(B6)}$$

It may also be noted that for zero angle of attack, the coefficients for the upper and lower surfaces are equal and thus the coefficients $L_{7,w}$, $kL_{8,w}$, $M'_{7,w}$, and $kM'_{8,w}$ are zero. Such would not be the case for nonzero angles of attack, however.

For pitch-axis locations other than $x_{o,w} = 0$, the transfer relations are found from the same procedure to be the conventional ones (e.g., see ref. 14) and are

$$\left.\begin{aligned}
L_{1,w} &= L'_{1,w} \\
L_{2,w} &= L'_{2,w} \\
L_{3,w} &= L'_{3,w} - 2x_{o,w}L_{1,w} \\
L_{4,w} &= L'_{4,w} - 2x_{o,w}L_{2,w} \\
L_{7,w} &= L'_{7,w} \\
L_{8,w} &= L'_{8,w}
\end{aligned}\right\} \qquad \text{(B7)}$$

and

$$
\left.
\begin{aligned}
M_{1,w} &= M'_{1,w} - 2x_{o,w}L_{1,w} \\
M_{2,w} &= M'_{2,w} - 2x_{o,w}L_{2,w} \\
M_{3,w} &= M'_{3,w} - 2x_{o,w}\left(M'_{1,w} + L'_{3,w} - 2x_{o,w}L_{1,w}\right) \\
M_{4,w} &= M'_{4,w} - 2x_{o,w}\left(M'_{2,w} + L'_{4,w} - 2x_{o,w}L_{2,w}\right) \\
M_{7,w} &= M'_{7,w} - 2x_{o,w}L_{7,w} \\
M_{8,w} &= M'_{8,w} - 2x_{o,w}L_{8,w}
\end{aligned}
\right\} \qquad \text{(B8)}
$$

APPENDIX C

DESCRIPTION OF COMPUTER PROGRAM

General Comments

A brief description of a FORTRAN computer program for numerically integrating the complex system of equations (7) to obtain the aerodynamic coefficients as a function of k is presented. A library routine INT2A for integrating a system of real, first-order, differential equations is used to integrate equations (7) after expanding into real form. The pitch and two translational motions are treated separately.

The program was written for use on the Control Data series 6000 computer systems using the Langley Research Center versions of the RUN compiler and SCOPE 3.0 operating system. Approximately 14 significant figures were used in the computations. The RUN compiler permits the use of multiple arithmetic statement on one card when separated by the character $. It might also be noted that the quantity 1777000000000000000_8 signifies an indefinite (undefined) quantity.

Input

Each case consists of a single card (80 characters) of identification for labeling the printout only and a list of variables in a NAMELIST called INPDATA. The FORTRAN variables and their definitions are as follows:

FORTRAN variable	Definition
XM	M_∞
THWD	Θ, degrees
G	γ
XOK	starting value of k for beginning numerical integration
XSTOPK	stopping value of k
CIK	k-increment for numerically integrating the differential equation
SPECK	k-increment for printing results

The input cards for the results presented in figure 10 are listed below:

```
********************************* COLUMN NUMBER ***********************************

00000000011111111112222222222333333333344444444445555555555666666666677777777778
12345678901234567890123456789012345678901234567890123456789012345678901234567890

FREQUENCY EFFECTS AT M=1000., GAMMA=1.4, SURFACE INCLINATION=25 DEG.
 $INPDATA G=1.4,XM=1000.,THWD=25.,XOK=.001,XSTOPK=1.,CIK=.001,SPECK=.01$
```

Output

The program lists each aerodynamic coefficient for each value of k requested (by SPECK) and the real and imaginary parts of the perturbation variables. The coefficients are also written on TAPE 7 in coded form for subsequent use by plotting programs.

Listing of Program

```
      OVERLAY(PF1STRP,0,0)
      PROGRAM PF1STRP(INPUT=1,OUTPUT,TAPE7,TAPE5=INPUT)
************************************************************************
*  PROGRAM PF1STRP CALCULATES THE UNSTEADY FORCES ON AN OSCILLATING,    *
*    INCLINED FLAT SURFACE IN A SUPERSONIC PERFECT GAS FLOW.            *
*    THE LINEARIZED PERTURBATIONS ABOUT THE MEAN STEADY FLOW ARE        *
*    CONSIDERED, WITH SOLUTION GIVEN BY A ONE-STRIP INTEGRAL METHOD.    *
*    TWICE THE FORCES AND MOMENTS FOR A SINGLE SURFACE ARE PRINTED.     *
************************************************************************
      COMMON/BLOCK1/CUVAR(9),DER(9),VAR(9),PDB,RODB,UDB,VDB,XM2S,XBOS,
     + RBOS,CVSR,CPLGI,CPTHI,CTNL2,DVSDXR,DVSDXI,RVDB,PDV,UDV,VDV,RCNL
     +,DRO,DIO
      DIMENSION IDENT(8),DATE(2),ELE1(8),ELE2(8),ERRVAL(8)
      EXTERNAL DERSUB,CHSUB
      NAMELIST/INPDATA/XM,THWD,G,XCK,XSTOPK,CIK,SPECK
C
  110 FORMAT(5E16.8)
  109  FORMAT(1H1//*  RIGID BODY FORE AND AFT TRANSLATION*)
  108 FORMAT(/7X*K*4X*KSQL3P*6X*KL4P*4X*KSQM3P*6X*KM4P*8X*BR*8X*BI*
     + 8X*PR*8X*PI*8X*UR*8X*UI*8X*DR*8X*DI*/)
  107  FORMAT(1H1//*  RIGID BODY PITCH*)
  106 FORMAT(/7X*K*7X*L1*7X*KL2*7X*M1P*6X*KM2P*8X*BR*8X*BI*
     + 8X*PR*8X*PI*8X*UR*8X*UI*8X*DR*8X*DI*/)
  105  FORMAT(1H1//*  RIGID BODY PLUNGE NORMAL TO SURFACE*)
  104 FORMAT(XF6.4,4G11.4,8G10.3)
  103 FORMAT(/7X*K*7X*L7*7X*KL8*7X*M7P*6X*KM8P*8X*BR*8X*BI*
     + 8X*PR*8X*PI*8X*UR*8X*UI*8X*DR*8X*DI*/)
  102 FORMAT(//*  PDB=*G16.8,* RODB=*G16.8,* UDB=*G16.8,* VDB=*G16.8
     +/*  PDV=*G16.8,* RODV=*G16.8,* UDV=*G16.8,* VDV=*G16.8/)
  101 FORMAT(/2X*M2=*G16.8,* P21=*G16.8,* R21=*G16.8,* V21=*G16.8,* BO=*
     +G16.8)
      DATA FMT1,FMT2,FMT3/6H(8A10),10H(1H110A10),10H(* IOB*I4)/
C
C  VAR(1,..,9)=X,BR,BI,PR,PI,UR,UI,DR,DI. RF=.5*V21*X
C
      REWIND 7
    1 READ FMT1,IDENT $ IF(EOF,5)999,2
    2 CALL DAYTIM(DATE) $ PRINT FMT2,IDENT,DATE $ READ INPDATA
      PRINT INPDATA $ THW=THWD/57.2957795130823
      CALL WEDGE(XM,G,THW,XM2,P21,R21,V21,BO,IEOBS)
      IF(IEOBS.EQ.0)GO TO 3 $ PRINT FMT3,IEOBS $ GO TO 1
    3 PRINT 101,XM2,P21,R21,V21,BO
      CALL SHKDERV(XM,G,THW,BO,R21,V21,PDV,RODV,UDV,VDV,PDB,RODB,UDB,
     + VDB) $ XM2S=XM2**2 $ XBOS=XM2S-1.
      PRINT 102,PDB,RODB,UDB,VDB,PDV,RODV,UDV,VDV $ PRINT 105
      RBOS=1./XBOS $ RVDB=1./VDB $ PCON=-R21*V21 $ CONM=PCON/3.
      CONTM=-2.*R21/3. $ XO=2.*XOK/V21 $ XSTOP=2.*XSTOPK/V21
      CI=2.*CIK/V21 $ SPEC=2.*SPECK/V21
```

```
C
C RIGID BODY PLUNGE
C
      CVSR=0. $ CPLGI=-1. $ CPTHI=0. $ II=0 $ DRO=-COS(BO-THW) $ DIO=0.
      CALL INIC(DPDXR,DPDXI,XO,THW,BO,PROO,PIOO,TNL) $ CTNL2=2./TNL
      CL1O=-R21*DPDXR $ CM1PO=4.*CL1O/3. $ CKL2O=PCON*PIOO $ XK=0.
      WRITE(7,110)XK,CL1O,CKL2O,CM1PO,CKL2O
      PRINT 106 $PRINT104,XK,CL1O,CKL2O,CM1PO,CKL2O
      CALL INT2A(II,8,DUM,CI,SPEC,DUM,DUM,VAR,CUVAR,DER,ELE1,ELE2,DUM,
     + ERRVAL,DERSUB,CHSUB,DUM)  $ XOO=VAR(1)
      CL1=-R21*(PROO+VAR(4))/XOO $ CKL2=.5*PCON*(PIOO+VAR(5))
      CM1P=CONTM*(PRCO+2.*VAR(4))/XOO $ CKM2P=CONM*(PIOO+2.*VAR(5))
      XSAV=VAR(1) $ PRSAV=VAR(4) $ PISAV=VAR(5) $ XK=.5*V21*VAR(1)
      WRITE(7,110)XK,CL1,CKL2,CM1P,CKM2P
      PRINT 104,XK,CL1,CKL2,CM1P,CKM2P,(VAR(I),I=2,9)  $ II=1
    7 CALL INT2A(II,8,DUM,CI,SPEC,DUM,DUM,VAR,CUVAR,DER,ELE1,ELE2,DUM,
     + ERRVAL,DERSUB,CHSUB,DUM)
      XS=VAR(1) $ RXSQ=1./XS**2 $ DX=XS-XSAV
      RX=XSAV/XS $ RX2=RX*RX $ RX3=RX2*RX
      CL1  =RX2*CL1-R21*DX*(PRSAV+VAR(4))*RXSQ
      CKL2=RX*CKL2+.5*PCON*DX*(PISAV+VAR(5))/XS
      TX1=VAR(1)+2.*XSAV $ TX2=2.*VAR(1)+XSAV
      CKM2P=RX2*CKM2P+CONM*RXSQ*DX*(TX1*PISAV+TX2*VAR(5))
      CM1P=RX3*CM1P+CONTM*RXSQ*DX*(TX1*PRSAV+TX2*VAR(4))/XS
      XSAV=VAR(1) $ PRSAV=VAR(4) $ PISAV=VAR(5) $ XK=.5*V21*VAR(1)
      WRITE(7,110)XK,CL1,CKL2,CM1P,CKM2P
      PRINT 104,XK,CL1,CKL2,CM1P,CKM2P,(VAR(I),I=2,9)
      IF(XS.LT.XSTOP)GO TO 7 $ ENDFILE 7 $ PRINT 109
C
C RIGID BODY FORE AND AFT TRANSLATION
C
      CVSR=CPLGI=CPTHI=DIO=0. $ II=0 $ DRO=SIN(BO-THW)
      CALL INIC(DPDXR,DPDXI,XO,THW,BO,PROO,PIOO,TNL) $ PRINT 103
      CL7O=-R21*DPDXR $ CM7PO=4.*CL7O/3. $ CKL8O=PCON*PIOO $ XK=0.
      WRITE(7,110)XK,CL7O,CKL8O,CM7PO,CKL8O
      PRINT 104,XK,CL7O,CKL8O,CM7PO,CKL8O
      CALL INT2A(II,8,DUM,CI,SPEC,DUM,DUM,VAR,CUVAR,DER,ELE1,ELE2,DUM,
     + ERRVAL,DERSUB,CHSUB,DUM)  $ XOO=VAR(1)
      CL7=-R21*(PROO+VAR(4))/XOO $ CKL8=.5*PCON*(PIOO+VAR(5))
      CM7P=CONTM*(PRCO+2.*VAR(4))/XOO$ CKM8P=CONM*(PIOO+2.*VAR(5))
      XSAV=VAR(1) $ PRSAV=VAR(4) $ PISAV=VAR(5) $ XK=.5*V21*VAR(1)
      WRITE(7,110)XK,CL7,CKL8,CM7P,CKM8P
      PRINT 104,XK,CL7,CKL8,CM7P,CKM8P,(VAR(I),I=2,9)  $ II=1
    8 CALL INT2A(II,8,DUM,CI,SPEC,DUM,DUM,VAR,CUVAR,DER,ELE1,ELE2,DUM,
     + ERRVAL,DERSUB,CHSUB,DUM)
      XS=VAR(1) $ RXSQ=1./XS**2 $ DX=XS-XSAV
      RX=XSAV/XS $ RX2=RX*RX $ RX3=RX2*RX
      CL7=RX2*CL7-R21*DX*(PRSAV+VAR(4))*RXSQ
      CKL8=RX*CKL8+.5*PCON*DX*(PISAV+VAR(5))/XS
      TX1=VAR(1)+2.*XSAV $ TX2=2.*VAR(1)+XSAV
      CKM8P=RX2*CKM8P+CONM*RXSQ*DX*(TX1*PISAV+TX2*VAR(5))
      CM7P=RX3*CM7P+CONTM*RXSQ*DX*(TX1*PRSAV+TX2*VAR(4))/XS
      XSAV=VAR(1) $ PRSAV=VAR(4) $ PISAV=VAR(5) $ XK=.5*V21*VAR(1)
      WRITE(7,110)XK,CL7,CKL8,CM7P,CKM8P
      PRINT 104,XK,CL7,CKL8,CM7P,CKM8P,(VAR(I),I=2,9)
      IF(XS.LT.XSTOP)GO TO 8 $ ENDFILE 7 $ PRINT 107
```

```
C
C RIGID BODY PITCH
C
      CVSR=-1. $ CPLGI=0. $ CPTHI=-1.  $ II=0 $ DRO=DIO=0.
      CALL INIC(DPDXR,DPDXI,XO,THW,BO,PROO,PIOO,TNL)$ PRINT 108
      CKSL3PO=V21*PCON*PROO $CKL4PO=PCON*DPDXI $CKM4PO=4.*CKL4PO/3.
      XK=0. $ WRITE(7,110)XK,CKSL3PO,CKL4PO,CKSL3PO,CKM4PO
      PRINT 104,XK,CKSL3PO,CKL4PO,CKSL3PO,CKM4PO
      CALL INT2A(II,8,DUM,CI,SPEC,DUM,DUM,VAR,CUVAR,DER,ELE1,ELE2,DUM,
     + ERRVAL,DERSUB,CHSUB,DUM)  $ XOO=VAR(1)
      CKSL3P=.5*PCON*V21*(PROO+VAR(4)) $ CKL4P=PCON*(PIOO+VAR(5))/XOO
      CKSM3P=CONM*V21*(PROO+2.*VAR(4))
      CKM4P=2.*CONM*(PIOO+2.*VAR(5))/XOO
      XSAV=VAR(1) $ PRSAV=VAR(4) $ PISAV=VAR(5) $ XK=.5*V21*VAR(1)
      WRITE(7,110)XK,CKSL3P,CKL4P,CKSM3P,CKM4P
      PRINT 104,XK,CKSL3P,CKL4P,CKSM3P,CKM4P,(VAR(I),I=2,9) $ II=1
    9 CALL INT2A(II,8,DUM,CI,SPEC,DUM,DUM,VAR,CUVAR,DER,ELE1,ELE2,DUM,
     + ERRVAL,DERSUB,CHSUB,DUM)
      XS=VAR(1) $ RXSQ=1./XS**2 $ DX=XS-XSAV
      RX=XSAV/XS $ RX2=RX*RX $ RX3=RX2*RX
      CKSL3P=RX*CKSL3P+.5*DX*V21*PCON*(PRSAV+VAR(4))/XS
      CKL4P=RX2*CKL4P +DX*RXSQ*PCON*(PISAV+VAR(5))
      TX1=VAR(1)+2.*XSAV $ TX2=2.*VAR(1)+XSAV
      CKSM3P=RX2*CKSM3P+CONM*V21*RXSQ*DX*(TX1*PRSAV+TX2*VAR(4))
      CKM4P=RX3*CKM4P +2.*CONM*RXSQ*DX*(TX1*PISAV+TX2*VAR(5))/XS
      XSAV=VAR(1) $ PRSAV=VAR(4) $ PISAV=VAR(5) $ XK=.5*V21*VAR(1)
      PRINT 104,XK,CKSL3P,CKL4P,CKSM3P,CKM4P,(VAR(I),I=2,9)
      WRITE(7,110)XK,CKSL3P,CKL4P,CKSM3P,CKM4P
      IF(XS.LT.XSTOP)GO TO 9 $ ENDFILE 7 $ GO TO 1
  999 REWIND 7
      END             PROGRAM PF1STRP
```

```
      SUBROUTINE INIC(DPDXR,DPDXI,XO,THW,BO,PRO,PIO,TNL)
*****************************************************************************
*  SUBROUTINE INIC CALCULATES THE INITIAL VALUES AND DERIVATIVES FOR     *
*    BEGINNING THE NUMERICAL INTEGRATION AT XO.                          *
*****************************************************************************
      COMMON/BLOCK1/CUVAR(9),DER(9),VAR(9),PDB,RODB,UDB,VDB,XM2S,XBOS,
     + RBOS,CVSR,CPLGI,CPTHI,CTNL2,DVSDXR,DVSDXI,RVDB,PDV,UDV,VDV,RCNL
     +,DRO,DIO
      VSR=CVSR          $  VSI=CPLGI        $ DVSDXI=CPTHI     $ DVSDXR=0.
      TNL=TAN(BO-THW) $  SNL=SIN(BO-THW) $ CNL=COS(BO-THW) $ RCNL=1./CNL
      BRO=(VSR+VDV*DIO)/VDB $ PRO=PDB*BRO-PDV*DIO
      BIO=(VSI-VDV*DRO)/VDB $ PIO=PDB*BIO+PDV*DRO
      URO=UDB*BRO-UDV*DIO $ UIO=UDB*BIO+UDV*DRO
      PRINT 1,VSR,VSI,BRO,BIO,PRO,PIO,URO,UIO,DRO,DIO
    1 FORMAT(/*  VSR=*G16.8,* VSI=*G16.8,* BRO=*G16.8,* BIO=*G16.8/
     +       *  PRO=*G16.8,* PIO=*G16.8,* URO=*G16.8,* UIO=*G16.8/,
     +       *  DRO=*G16.8,* DIO=*G16.8/)
      BNUM1=1.-XBOS*TNL*TNL $ BNUM2=.5*XBOS*TNL*TNL
      BNUM3=TNL*(XM2S*PDV-UDV+.5*VDV*XBOS*TNL)
      BNUM4=TNL*(XM2S*PDB-UDB+VDV/SNL+.5*XBOS*TNL*(VDB+2.*PDV/SNL))
      DENOM=VDB+XBOS*TNL*PDB
      DBDXR=(BNUM1*DVSDXR+BNUM2*VSI+BNUM3*DRO+BNUM4*BIO)/DENOM
      DBDXI=(BNUM1*DVSDXI-BNUM2*VSR+BNUM3*DIO-BNUM4*BRO)/DENOM
      DPDXR=PDB*DBDXR+TNL*(DVSDXR-.5*(VSI+VDV*DRO+BIO*(VDB+2.*PDV/SNL)))
      DPDXI=PDB*DBDXI+TNL*(DVSDXI+.5*(VSR-VDV*DIO+BRO*(VDB+2.*PDV/SNL)))
      DUDXR=-DPDXR+UIO $ DUDXI=-DPDXI-URO
      PRINT 2,DBDXR,DBDXI,DPDXR,DPDXI,DUDXR,DUDXI
    2 FORMAT(* DBDXR=*G16.8,* DBDXI=*G16.8,* DPDXR=*G16.8,* DPDXI=*G16.8
     +,/      * DUDXR=*G16.8,* DUDXI=*G16.8/)
      VAR(2)=BRO+XO*DBDXR $ VAR(3)=BIO+XO*DBDXI $ VAR(1)=XO
      VAR(4)=PRO+XO*DPDXR $ VAR(5)=PIO+XO*DPDXI
      VAR(6)=URO+XO*DUDXR $ VAR(7)=UIO+XO*DUDXI
      VAR(8)=DRO+XO*BRO*RCNL $ VAR(9)=DIO+XO*BIO*RCNL $ RETURN
      END             SUBROUTINE INIC

      SUBROUTINE CHSUB $ RETURN
*****************************************************************************
*  DUMMY SUBROUTINE CALLED BY INT2A.                                        *
*****************************************************************************
      END             SUBROUTINE CHSUB
```

```
      SUBROUTINE DERSUB
*****************************************************************************
*  SUBROUTINE DERSUB CALCULATES THE FIRST ORDER DERIVATIVES FOR EACH     *
*    STEP OF THE NUMERICAL INTERGRATION.  DERSUB IS CALLED BY INT2A.     *
*****************************************************************************
      COMMON/BLOCK1/CUVAR(9),DER(9),VAR(9),PDB,RODB,UDB,VDB,XM2S,XBOS,
     + RBOS,CVSR,CPLGI,CPTHI,CTNL2,DVSDXR,DVSDXI,RVDB,PDV,UDV,VDV,RCNL
     +,DRO,DIO
      X= CUVAR(1) $ BR=CUVAR(2) $ BI=CUVAR(3) $ PR=CUVAR(4)
      PI=CUVAR(5) $ UR=CUVAR(6) $ UI=CUVAR(7) $ DR=CUVAR(8) $DI=CUVAR(9)
      VSR=CVSR     $ VSI=(CPLGI+X*CPTHI)     $ RX=1./X
      DER(2)=((VDB*BR+CTNL2*(PR-PDB*BR)+(CTNL2*PDV-VDV)*DI-VSR)*RX
     1 -DVSDXR+((VDB+VDV*RCNL)*BI+VSI+VDV*DR))*RVDB
      DER(3)=((VDB*BI+CTNL2*(PI-PDB*BI)-(CTNL2*PDV-VDV)*DR-VSI)*RX
     1 -DVSDXI-((VDB+VDV*RCNL)*BR+VSR-VDV*DI))*RVDB
      DER(4)=(RX*(CTNL2*VSR+(CTNL2*VDV-XBOS*PDV)*DI+(PDB*XBOS-VDB*
     1 CTNL2)*BR-XBOS*PR)-XBOS*PDB*DER(2)+((PDV*XM2S-UDV)*DR-UI
     2 +XM2S*PI+(PDB*XM2S-UDB+XBOS*PDV*RCNL)*BI))*RBOS
      DER(5)=(RX*(CTNL2*VSI-(CTNL2*VDV-XBOS*PDV)*DR+(PDB*XBOS-VDB*
     1 CTNL2)*BI-XBOS*PI)-XBOS*PDB*DER(3)+((PDV*XM2S-UDV)*DI+UR
     2 -XM2S*PR-(PDB*XM2S-UDB+XBOS*PDV*RCNL)*BR))*RBOS
      DER(6)=RX*((PDB+UDB)*BR-PR-UR-(PDV+UDV)*DI)-DER(4)
     1 -(PDB+UDB)*DER(2)+(UI+(UDB+(UDV+PDV)*RCNL)*BI+UDV*DR)
      DER(7)=RX*((PDB+UDB)*BI-PI-UI+(PDV+UDV)*DR)-DER(5)
     1 -(PDB+UDB)*DER(3)-(UR+(UDB+(UDV+PDV)*RCNL)*BR-UDV*DI)
      DER(8)=BR*RCNL $ DER(9)=BI*RCNL $ RETURN
      END            SUBROUTINE DERSUB


      SUBROUTINE SHKDERV(XM,G,THW,BO,ROO,UO,PV,ROV,UV,VV,PB,ROB,UB,VB)
*****************************************************************************
*  CALCULATES SLOPE AND NORMAL VELOCITY DERIVATIVES OF P,RO,U, AND V FOR*
*    AN OBLIQUE SHOCK WAVE. DERIVATIVES ARE NORMALIZED BY FLOW VARIABLES*
*    BEHIND THE SHOCK WAVE.                                             *
*****************************************************************************
      SLO=SIN(BO-THW) $ CLO=COS(BO-THW) $ SB=SIN(BO) $ CB=COS(BO)
      SQMN=(XM*SB)**2 $ FG1=4./(G+1.)    $ RUO=1./UO
      PN= FG1*SB*RUO  $ PV=PN/ROO        $ PB=PV*CB*RUO
      ROV=FG1*ROO/(SQMN*SB)          $ ROB=ROV*CB
      UN=.5*FG1*(SQMN+1.)/SQMN       $ UB=UN*RUO*SIN(THW)-PN*CLO
      UV=-UN*SLO       $ VV=UN*CLO   $ VB=UN*RUO*COS(THW)-PN*SLO
      RETURN
      END            SUBROUTINE SHKDERV
```

```
      SUBROUTINE WEDGE(XM,G,THW,XM2,P2OP1,R2OR1,V2OV1,BETAO,IER)
*************************************************************************
*  CALCULATES SHOCK WAVE ANGLE BETAO (RADIANS) FOR A WEDGE OF ANGLE     *
*    THETA (RADIANS) FOR INPUT VALUES OF MACH NUMBER XM AND GAMMA G -   *
*    FLOW CONDITIONS BEHIND THE SHOCK ARE CALCULATED FROM BETAO,XM,AND G*
*************************************************************************
      RINDF=01777C00000000000017 $ IF(XM.GE.1.)GO TO 1$ IER=1 $ GO TO 9
    1 IF(THW)8,7,2
    2 STSQ=SIN(THW)**2 $ SQM=XM*XM $ RSQM=1./SQM
      B=-RSQM*(SQM+2.)-G*STSQ      $ D=(STSQ-1.)*RSQM**2
      C=(2.*SQM+1.)*RSQM**2+(.25*(G*(G+2.)+1.)+RSQM*(G-1.))*STSQ
      CALL WDETACH(XM,G,TDET) $ IF(THW.LE.TDET)GO TO 3 $ IER=3 $ GO TO 9
    3 X=-.333333333333333*B        $ TCORR=1. $ DO 4 I=1,100
      CORR=-(D+X*(C+X*(B+X)))/(C+X*(2.*B+3.*X)) $ XT=X $ X=X+CORR
      IF(I.NE.1.AND.(TCORR*CORR.LE.0..OR.X.EQ.XT))GO TO 5
    4 TCORR=CORR $ IER=4           $ SMN=X*SQM $ GO TO 6
    5 IER=0       $ SMN=X*SQM
    6 P2OP1=(2.*G*SMN-G+1.)/(G+1.) $ R2OR1=(G+1.)*SMN/(2.+SMN*(G-1.))
      V2OV1=SQRT(1.-4.*(SMN-1.)*(G*SMN+1.)/(SMN*SQM*(G*(G+2.)+1.)))
      XM2=XM*V2OV1*SQRT(R2OR1/P2OP1) $ BETAO=ASIN(SQRT(X))       $ RETURN
    7 P2OP1=R2OR1=V2OV1=1. $ XM2=XM $ BETAO=ASIN(1./XM) $ IER=0 $ RETURN
    8 IER=2
    9 P2OP1=R2OR1=V2OV1=BETAO=XM2=RINDF $ RETURN
      END            SUBROUTINE WEDGE

      SUBROUTINE WDETACH(XM,G,DEL) $ XMS=XM*XM $ GP=G+1.
*************************************************************************
*  CALCULATES WEDGE ANGLE FOR SHOCK DETACHMENT DEL (RADIANS) FOR INPUT  *
*    VALUES OF MACH NUMBER XM AND GAMMA G                               *
*************************************************************************
      XMNS=.25*(GP*XMS-4.+SQRT(GP*(XMS*(GP*XMS+8.*(G-1.))+16.)))/G
      SINDEL=SQRT((XMS-XMNS*(2.*XMS+1.-XMNS*(XMS+2.-XMNS)))/
     +(1.+XMNS*(G-1.+.25*XMS*GP*GP-G*XMNS)))/XM$ DEL=ASIN(SINDEL)$RETURN
       END           SUBROUTINE WDETACH
```

```
      SUBROUTINE INT2A(II,N,NT,CI,SPEC,CIMAX, IERR ,VAR,CUVAR,DER,ELE1,
     1ELE2,ELT,ERRVAL,DERSUB,CHKSUB,ITEXT)
**********************************************************************
*     VERSION OF LRC CDC 6600 LIBRARY ROUTINE D2.4                   *
*     USES FIXED INTERVAL, SINGLE PRECISION, 4TH-ORDER ADAMS-BASHFORTH   *
*     PREDICTOR, 4TH-ORDER ADAMS-MOULTON CORRECTOR, 4TH-ORDER RUNGE-     *
*     KUTTA STARTER.  NT,CIMAX,IERR,ELT, AND ITEXT ARE DUMMY (UNUSED).   *
**********************************************************************
      DIMENSION DER(21),ELE1(20),ELE2(20),ELT(20),ERRVAL(20),TEMP(20),
     1 DER1(20),DER2(20),DER3(20),S1VAR(21),VAR(21),CUVAR(21)
      A=0.0  $  IF(II)1,1,2
C     INITIALIZATION SECTION
    1 IF(CI) 3,4,3
C     SAVE CI
    4 PRINT 1000 $ STOP
 1000 FORMAT(11HOCI=0  STOP)
    3 H=CI
   18 IERR=1 $ TO = VAR(1) $ MODE=1 $ II= 1 $ N1=N+1 $ DO 5 J=1,N1
      CUVAR(J)=VAR(J)
    5 CONTINUE
C     EVALUATION SECTION HERE
    8 CALL DERSUB $ IF(MODE.LE.1)GO TO 7 $ IF(II-3)36,36,7
   36 CALL CHKSUB $ IF(II.EQ.2) GO TO 1
   37 DO 38 J=1,N1
   38 VAR(J)=CUVAR(J) $ IF(II-3)6,7,7
    7 RETURN
    6 IF(SPEC) 9,7,9
    9 DEL=     VAR(1) -TO $ DELP=DEL*(1.+1.0E-11)
      IF(ABS(DELP)-ABS(SPEC)) 2,10,10
   10 TO = VAR(1) $ GO TO 7
    2 II=1 $ IF(MODE-4) 11,12,12
C     RUNGE-KUTTA
   11 DO 20 J=2,N1 $ DER3(J-1)=DER2(J-1) $ DER2(J-1)=DER1(J-1)
      DER1(J-1)=DER(J) $ ELE1(J-1)=DER(J) $ CUVAR(J)=A
      DELT=0.4*ELE1(J-1)*H $ S1VAR(J)=VAR(J) $ CUVAR(J)=S1VAR(J)+DELT
   20 CONTINUE $ S1VAR(1)=VAR(1) $ CUVAR(1)=S1VAR(1)+0.4*H $ CALL DERSUB
```

```
      IF(II-3)23,23,7
   23 CUVAR(1)=S1VAR(1)+0.4557372542187 9*H $ DO 24 J=2,N1
      ELE2(J-1)=DER(J)
      DELT=(0.2969776092477 5*ELE1(J-1)+0.1587596449710 4*ELE2(J-1))*H
      CUVAR(J)=S1VAR(J)+DELT
   24 CONTINUE $ CALL DERSUB $ IF(II-3)25,25,7
   25 CUVAR(1)=S1VAR(1)+H $ DO 26 J=2,N1 $ TEMP(J-1)=DER(J)
      DELT=(0.2181003882259 2*ELE1(J-1)-3.0509651486929 3*ELE2(J-1)
     1+3.8328647604670 1*TEMP(J-1))*H $ CUVAR(J)=S1VAR(J)+DELT
   26 CONTINUE $ CALL DERSUB $ IF(II-3)27,27,7
   27 DH=H $ CUVAR(1)=VAR(1)+DH $ DO 28 J=2,N1
      DOUB=     (0.1747602822626 9*ELE1(J-1)-0.5514806628787 3*ELE2(J-1)
     1+1.2055355093965 2*TEMP(J-1)+0.1711847812195 2*DER(J))
      CUVAR(J)=VAR(J)+DH*DOUB
   28 CONTINUE $ MODE=MODE+1 $ GO TO 8
C     ADAMS-MOULTON, ADAMS-BASHFORTH PREDICTOR
   12 CUVAR(1)=VAR(1)+H $ DH=H/24.0 $ DO 13 J=2,N1
      DOUB=     (55.0*DER(J)-59.0*DER1(J-1)+37.0*DER2(J-1)-9.0*DER3(J-1))
      CUVAR(J)=VAR(J)+DH*DOUB
   13 CONTINUE $ DO 14 J=1,N $ DER3(J  )=DER2(J) $ DER2(J  )=DER1(J)
   14 DER1(J  )=DER(J+1) $ CALL DERSUB $ IF(II-3)15,15,7
C     ADAMS-MOULTON CORRECTOR
   15 DO 16 J=2,N1 $ TEMP=CUVAR(J)
      DOUB=     (9.0*DER(J)+19.*DER1(J-1)-5.0*DER2(J-1)+DER3(J-1))
      CUVAR(J)=VAR(J)+DH*DOUB
   16 ERRVAL(J-1)=(TEMP-     CUVAR(J)) /14.210526315798 47
   19 GO TO 8
      END            SUBROUTINE INT2A
```

REFERENCES

1. Moretti, Gino; and Abbett, Michael: A Time-Dependent Computational Method for Blunt Body Flows. AIAA J., vol. 4, no. 12, Dec. 1966, pp. 2136-2141.

2. Barnwell, Richard W.: A Time-Dependent Method for Calculating Supersonic Blunt-Body Flow Fields With Sharp Corners and Embedded Shock Waves. NASA TN D-6031, 1970.

3. Rakich, John V.: A Method of Characteristics for Steady Three-Dimensional Supersonic Flow With Application to Inclined Bodies of Revolution. NASA TN D-5341, 1969.

4. Belotserkovskiy, O. M.; and Chushkin, P. I.: The Numerical Method of Integral Relations. Zhurnal vychislitel'noy matematiki i matematicheskoy fiziki (J. Computational Mathematics and Mathematical Physics), vol. II, no. 5, Moscow, Sept.-Oct. 1962, pp. 731-759. (Also available as NASA TT F-8356.)

5. South, Jerry C., Jr.: Calculation of Axisymmetric Supersonic Flow Past Blunt Bodies With Sonic Corners, Including a Program Description and Listing. NASA TN D-4563, 1968.

6. George, A. R.: Perturbations of Plane and Axisymmetric Entropy Layers. AIAA J., vol. 5, no. 12, Dec. 1967, pp. 2155-2160.

7. South, J. C., Jr.; and Newman, P. A.: Supersonic Flow Past Pointed Bodies. AIAA J., vol. 3, no. 6, June 1965, pp. 1019-1021.

8. Ashley, Holt: Aeroelasticity. Appl. Mech. Rev., vol. 23, no. 2, Feb. 1970, pp. 119-129.

9. Wood, B. M.: A Survey of Unsteady Hypersonic Flow Problems. C.P. No. 901, Brit. A.R.C., 1966.

10. Ashley, Holt; and Zartarian, Garabed: Theoretical Hypervelocity Unsteady Aerodynamics. Proceedings of Symposium on Aerothermoelasticity, ASD TR 61-645, U.S. Air Force, Oct.-Nov. 1961, pp. 161-218.

11. Runyan, Harry L.; and Morgan, Homer G.: Flutter at Very High Speeds. NASA TN D-942, 1961. (Supersedes NACA RM L57D16a.)

12. Morgan, Homer G.; Runyan, Harry L.; and Huckel, Vera: Theoretical Considerations of Flutter at High Mach Numbers. J. Aeronaut. Sci., vol. 25, no. 6, June 1958, pp. 371-381.

13. Miles, John W.: Unsteady Flow at Hypersonic Speeds. Hypersonic Flow, A. R. Collar and J. Tinkler, eds., Academic Press, Inc., 1960, pp. 185-201.

14. Garrick, I. E.; and Rubinow, S. I.: Flutter and Oscillating Air-Force Calculations for an Airfoil in a Two-Dimensional Supersonic Flow. NACA Rep. 846, 1946. (Supersedes NACA TN 1158.)

15. Miles, John W.: The Potential Theory of Unsteady Supersonic Flow. Cambridge Univ. Press, 1959.

16. Donato, Vincent W.; and Huhn, Charles R., Jr.: Supersonic Unsteady Aerodynamics for Wings With Trailing Edge Control Surfaces and Folded Tips. AFFDL-TR-68-30, U.S. Air Force, Aug. 1968. (Available from DDC as AD 840 598.)

17. Hayes, Wallace D.: On Hypersonic Similitude. Quart. Appl. Math., vol. V, no. 1, Apr. 1947, pp. 105-106.

18. Lighthill, M. J.: Oscillating Airfoils at High Mach Number. J. Aeronaut. Sci., vol. 20, no. 6, June 1953, pp. 402-406.

19. Ashley, Holt; and Zartarian, Garabed: Piston Theory – A New Aerodynamic Tool for the Aeroelastician. J. Aeronaut. Sci., vol. 23, no. 12, Dec. 1956, pp. 1109-1118.

20. Chawla, Jagannath P.: Aeroelastic Instability at High Mach Number. J. Aeronaut. Sci., vol. 25, no. 4, Apr. 1958, pp. 246-258.

21. Morgan, Homer G.; Huckel, Vera; and Runyan, Harry L.: Procedure for Calculating Flutter at High Supersonic Speed Including Camber Deflections, and Comparison With Experimental Results. NACA TN 4335, 1958.

22. Van Dyke, Milton D.: A Study of Hypersonic Small-Disturbance Theory. NACA Rep. 1194, 1954. (Supersedes NACA TN 3173.)

23. Zartarian, Garabed; and Sauerwein, Harry: Further Studies on High-Speed Unsteady Flow. ASD-TDR-62-463, U.S. Air Force, Sept. 1962.

24. Aroesty, J.; Charwat, A. F.; Chen, S. Y.; and Cole, J. D.: Newtonian Snowplow Theory of Oscillating Airfoils. Mem. RM-4415-ARPA, RAND Corp., May 1966. (Available from DDC as AD 633 971.)

25. Yates, E. Carson, Jr.; and Bennett, Robert M.: Analysis of Supersonic-Hypersonic Flutter of Lifting Surfaces at Angle of Attack. AIAA Paper No. 71-327, Apr. 1971.

26. Carrier, G. F.: The Oscillating Wedge in a Supersonic Stream. J. Aeronaut. Sci., vol. 16, no. 3, Mar. 1949, pp. 150-152.

27. Van Dyke, Milton D.: On Supersonic Flow Past an Oscillating Wedge. Quart. Appl. Math., vol. XI, no. 3, Oct. 1953, pp. 360-363.

28. Carrier, G. F.: On the Stability of the Supersonic Flows Past a Wedge. Quart. Appl. Math., vol. VI, no. 4, Jan. 1949, pp. 367-378.

29. McIntosh, S. C., Jr.: Hypersonic Flow Over an Oscillating Wedge. AIAA J., vol. 3, no. 3, Mar. 1965, pp. 433-440.

30. McIntosh, Samuel Crutcher, Jr.: Studies in Unsteady Hypersonic Flow Theory. Ph. D. Diss., Stanford Univ., 1965.

31. Appleton, J. P.: Aerodynamic Pitching Derivatives of a Wedge in Hypersonic Flow. AIAA J., vol. 2, no. 11, Nov. 1964, pp. 2034-2036.

32. Bailie, J. A.; and McFeely, J. E.: Binary Flutter of Wedges in Hypersonic Flow. J. Spacecraft Rockets, vol. 3, no. 7, July 1966, pp. 1130-1132.

33. Orlik-Rückemann, K. J.: Effect of Wave Reflections on the Unsteady Hypersonic Flow Over a Wedge. AIAA J., vol. 4, no. 10, Oct. 1966, pp. 1884-1886.

34. Kuiken, H. K.: Large-Amplitude Low-Frequency Oscillation of a Slender Wedge in Inviscid Hypersonic Flow. AIAA J., vol. 7, no. 9, Sept. 1969, pp. 1767-1774.

35. Orlik-Rückemann, K. J.: Simple Formulas for Unsteady Pressure on Slender Wedges and Cones in Hypersonic Flow. J. Spacecraft Rockets, vol. 6, no. 10, Oct. 1969, pp. 1209-1211.

36. Hui, Wai How: Stability of Oscillating Wedges and Caret Wings in Hypersonic and Supersonic Flows. AIAA J., vol. 7, no. 8, Aug. 1969, pp. 1524-1530.

37. Hui, Wai How: Interaction of a Strong Shock With Mach Waves in Unsteady Flow. AIAA J., vol. 7, no. 8, Aug. 1969, pp. 1605-1607.

38. Hui, W. H.: Large-Amplitude Slow Oscillation of Wedges in Inviscid Hypersonic and Supersonic Flows. AIAA J., vol. 8, no. 8, Aug. 1970, pp. 1530-1532.

39. Kacprzynski, J. J.: A Low Frequency Solution of Unsteady Inviscid Hypersonic Flow Past an Oscillating Wedge With Attached Shock Wave. LTR-UA-5, Nat. Aeronaut. Estab. Canada, Sept. 1968.

40. Bailie, J. A.; and McFeely, J. E.: Panel Flutter in Hypersonic Flow. AIAA J., vol. 6, no. 2, Feb. 1968, pp. 332-337.

41. Brong, E. A.: The Flow Field About a Right Circular Cone in Unsteady Flight. AIAA Paper No. 65-398, July 1965.

42. Pugh, P. G.; and Woodgate, L.: Measurements of Pitching-Moment Derivatives for Blunt-Nosed Aerofoils Oscillating in Two-Dimensional Supersonic Flow. R. & M. No. 3315, Brit. A.R.C., 1963.

43. Liepmann, H. W.; and Roshko, A.: Elements of Gasdynamics. John Wiley & Sons, Inc., c.1957.

44. Van Dyke, Milton D.: Supersonic Flow Past Oscillating Airfoils Including Nonlinear Thickness Effects. NACA Rep. 1183, 1954. (Supersedes NACA TN 2982.)

45. Ames Research Staff: Equations, Tables, and Charts for Compressible Flow. NACA Rep. 1135, 1953. (Supersedes NACA TN 1428.)

46. South, Jerry C., Jr.: Application of Dorodnitsyn's Integral Method to Nonequilibrium Flows Over Pointed Bodies. NASA TN D-1942, 1963.

47. Johnston, G. W.: An Investigation of the Flow About Cones and Wedges at and Beyond the Critical Angle. J. Aeronaut. Sci., vol. 20, no. 6, June 1953, pp. 378-382.

48. Landahl, Mårten T.: Unsteady Transonic Flow. Pergamon Press, Inc., 1961.

49. Lambourne, N. C.: Calculations Showing the Influence of Aerodynamic Damping on Binary Wing Flutter. R. & M. No. 3579, Brit. A.R.C., 1969.

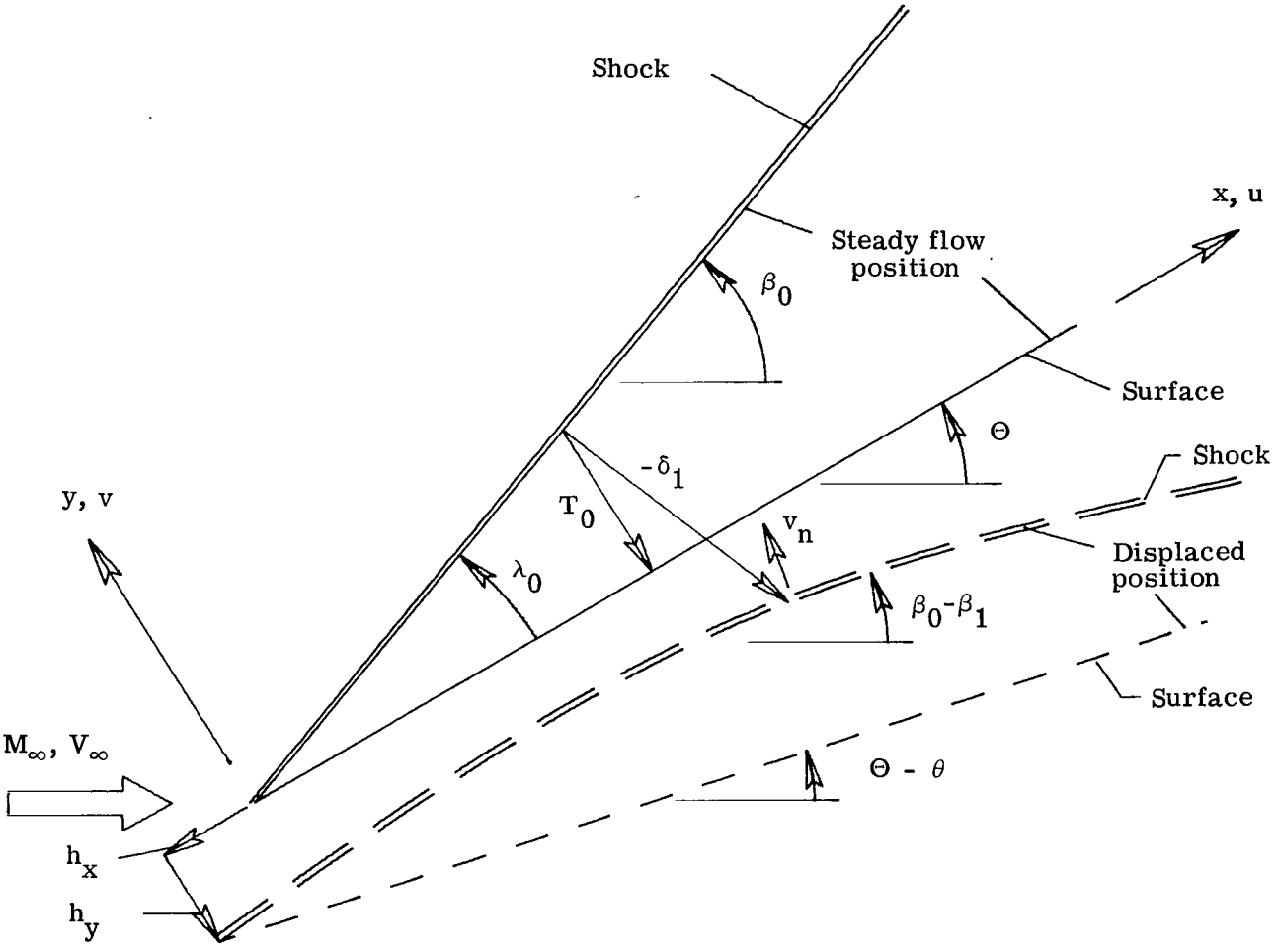

Figure 1.- Oscillating flat surface and coordinate system.

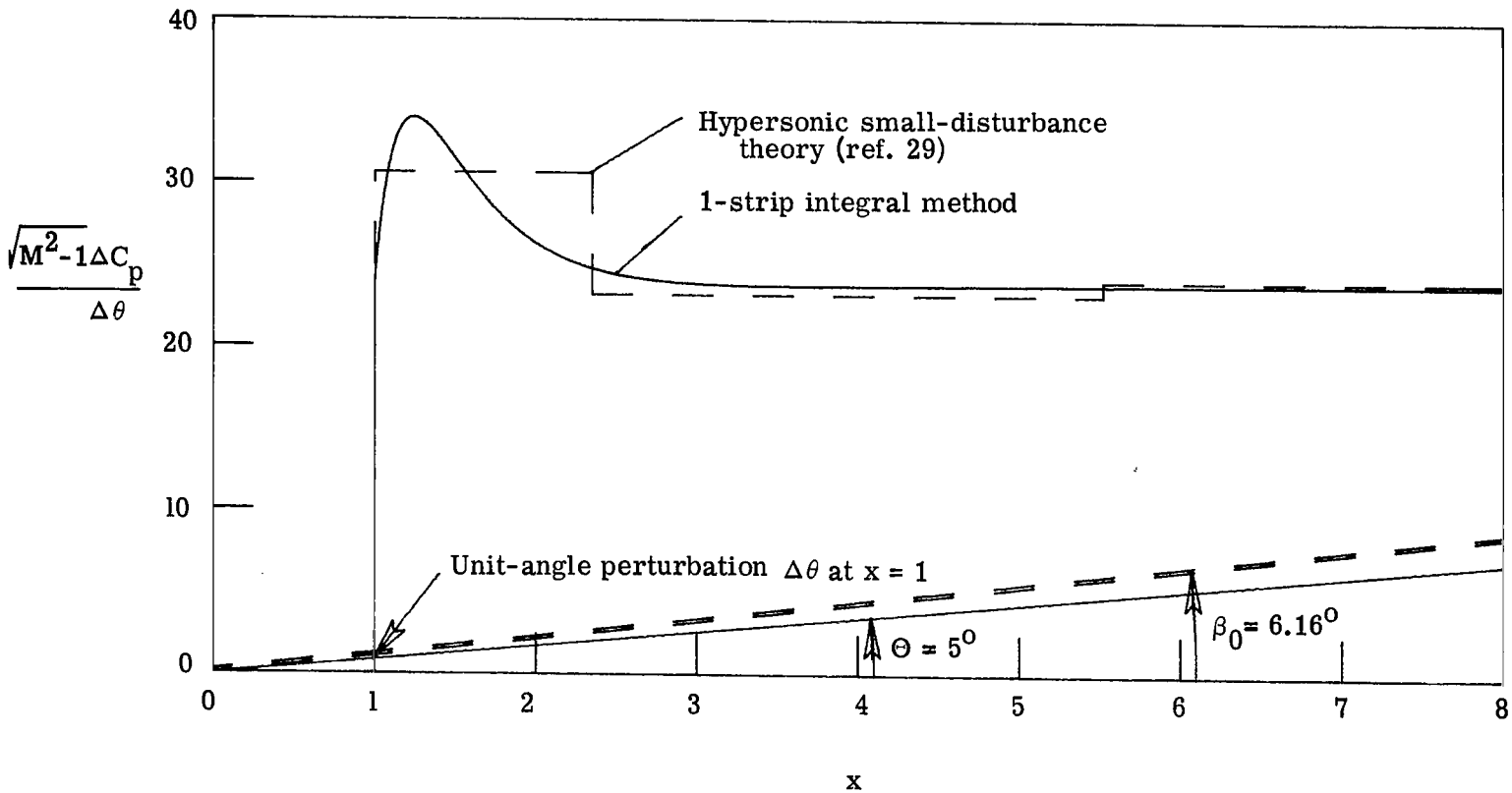

Figure 2.- Pressure perturbation downstream of a unit-angle perturbation. Mach 57.3.

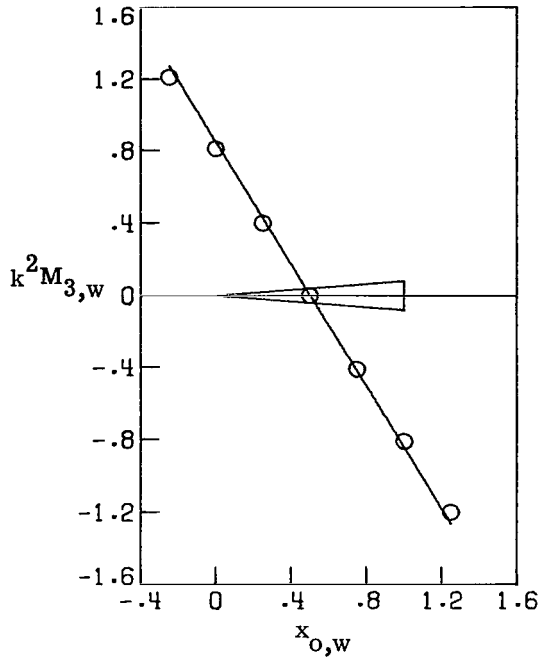

(a) $\tau = 0.16$; Mach 1.75.

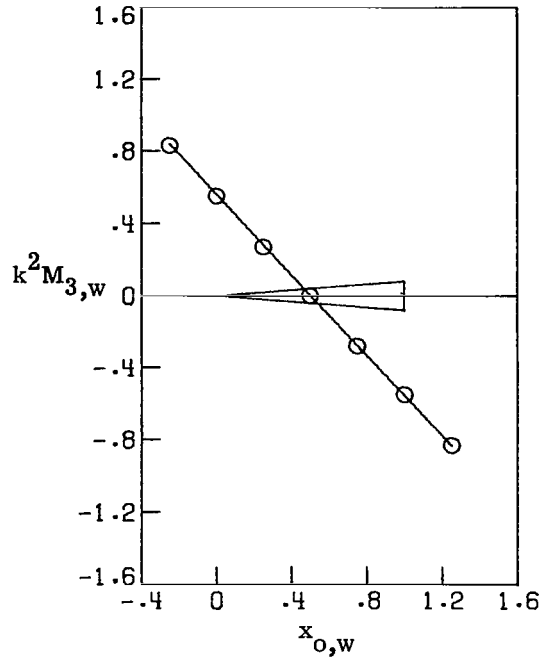

(b) $\tau = 0.16$; Mach 2.47.

——— 1-strip integral method
○ Experiment (ref. 42)

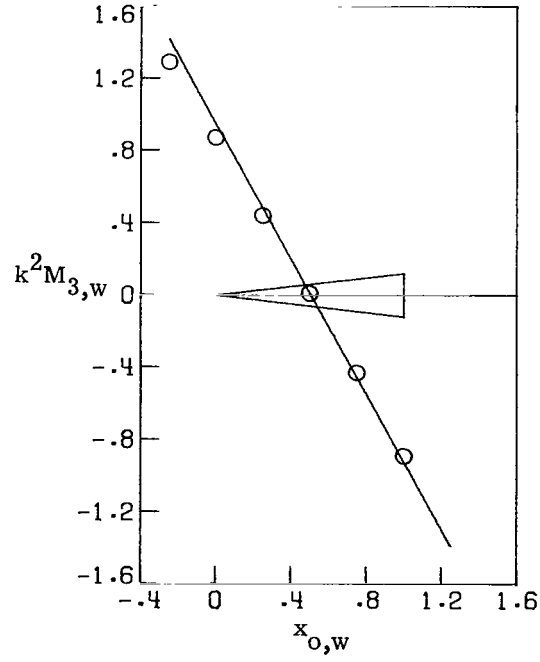

(c) $\tau = 0.24$; Mach 1.75.

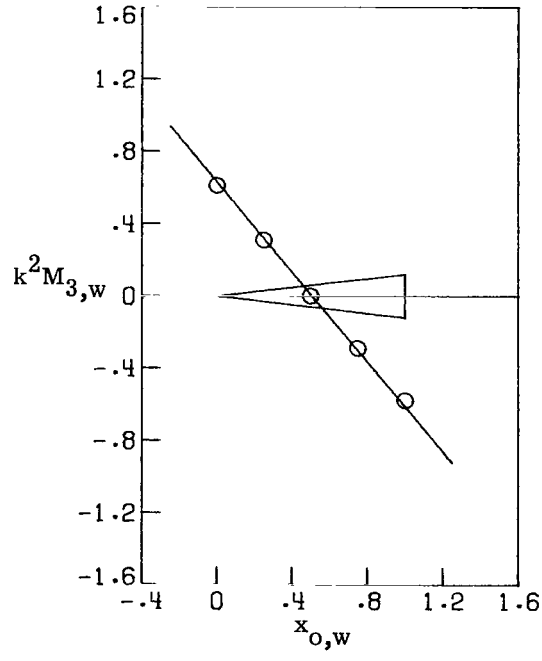

(d) $\tau = 0.24$; Mach 2.47.

Figure 3.- Variation of static moment derivative with pitch-axis location.

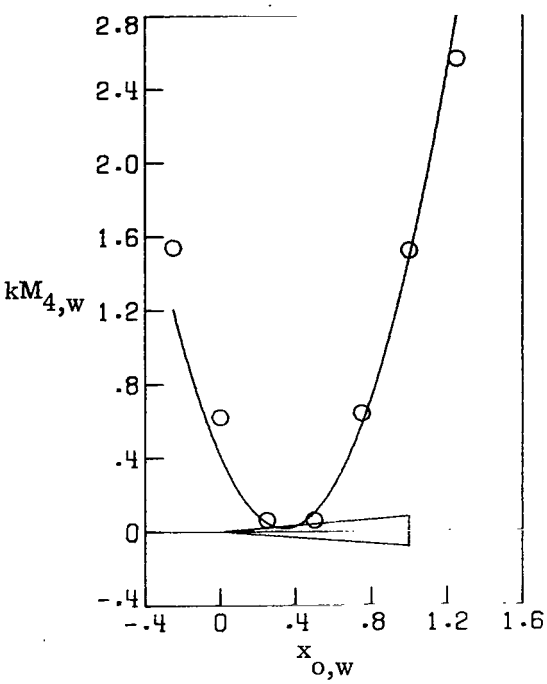

(a) $\tau = 0.16$; Mach 1.75.

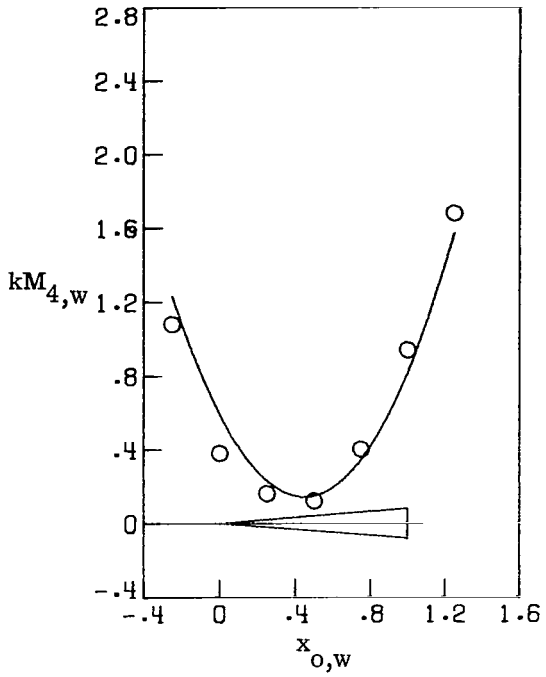

(b) $\tau = 0.16$; Mach 2.47.

—— 1-strip integral method
○ Experiment (ref. 42)

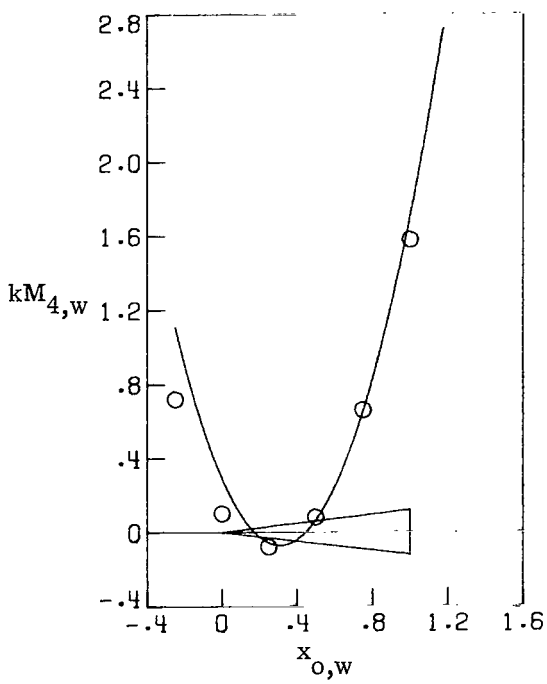

(c) $\tau = 0.24$; Mach 1.75.

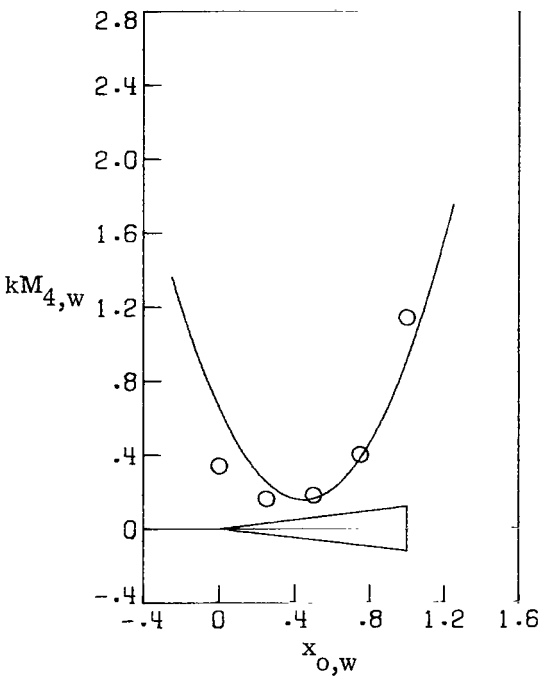

(d) $\tau = 0.24$; Mach 2.47.

Figure 4.- Variation of pitch-rate-damping moment derivative with pitch-axis location.

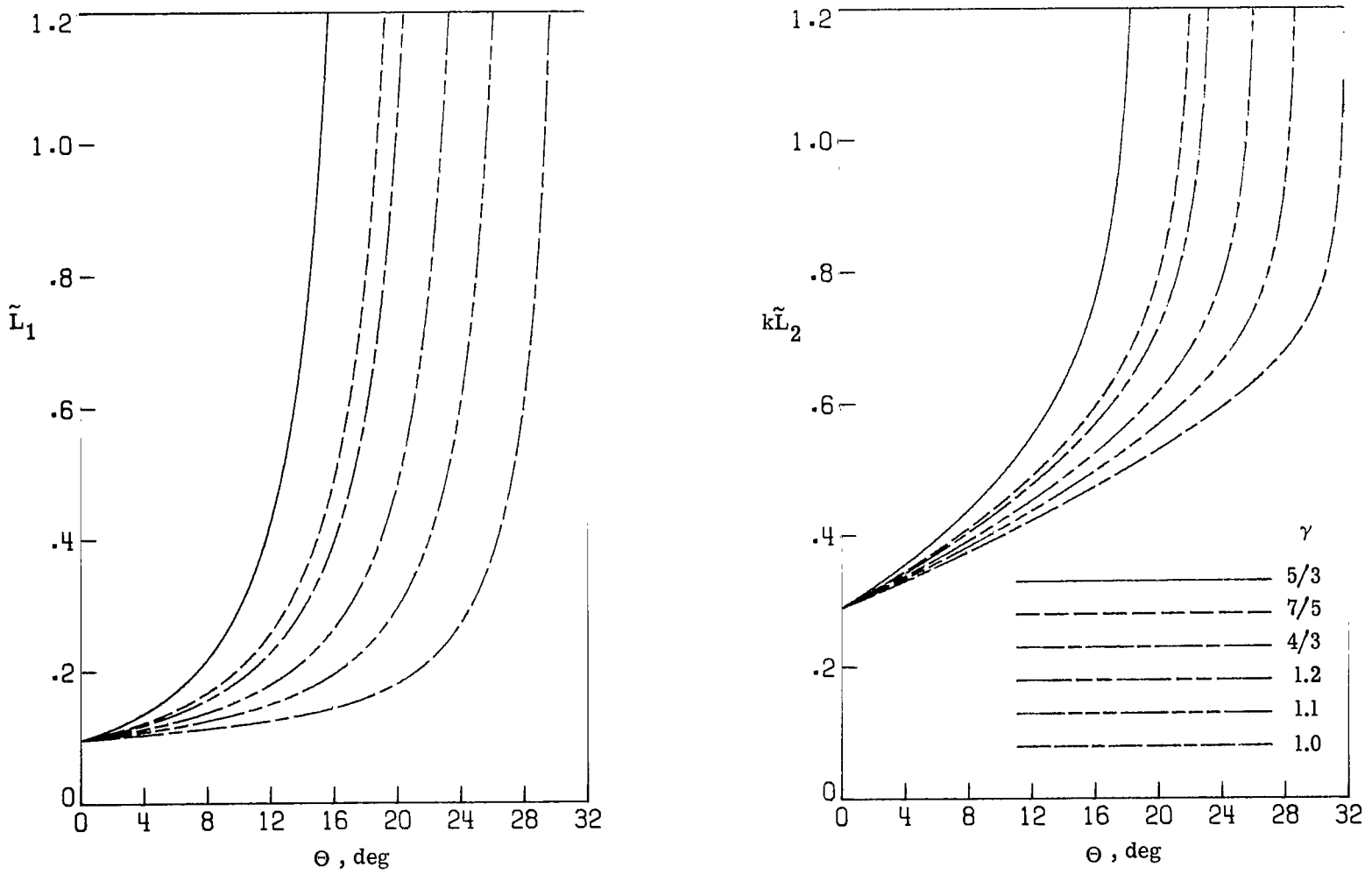

Figure 5.- Coefficients for a single surface at a Mach number of 2. k = 0.

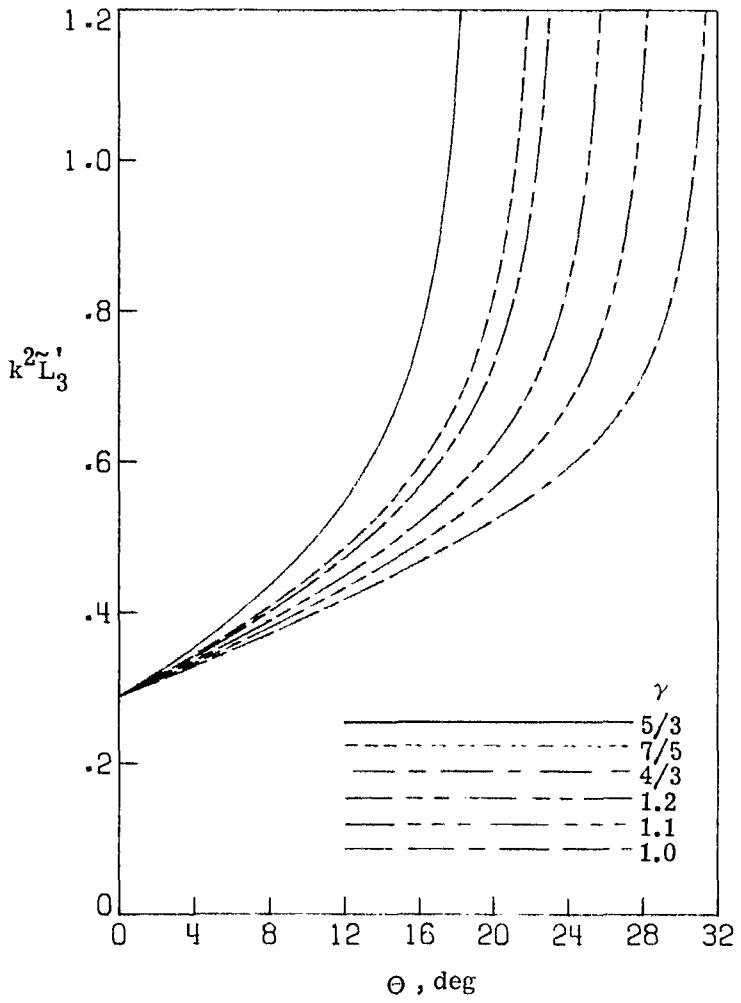

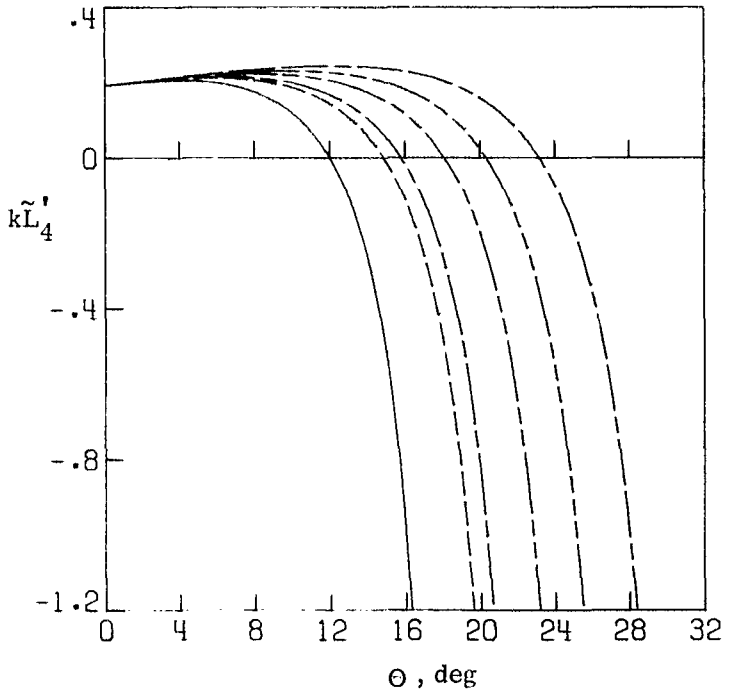

Figure 5.- Continued.

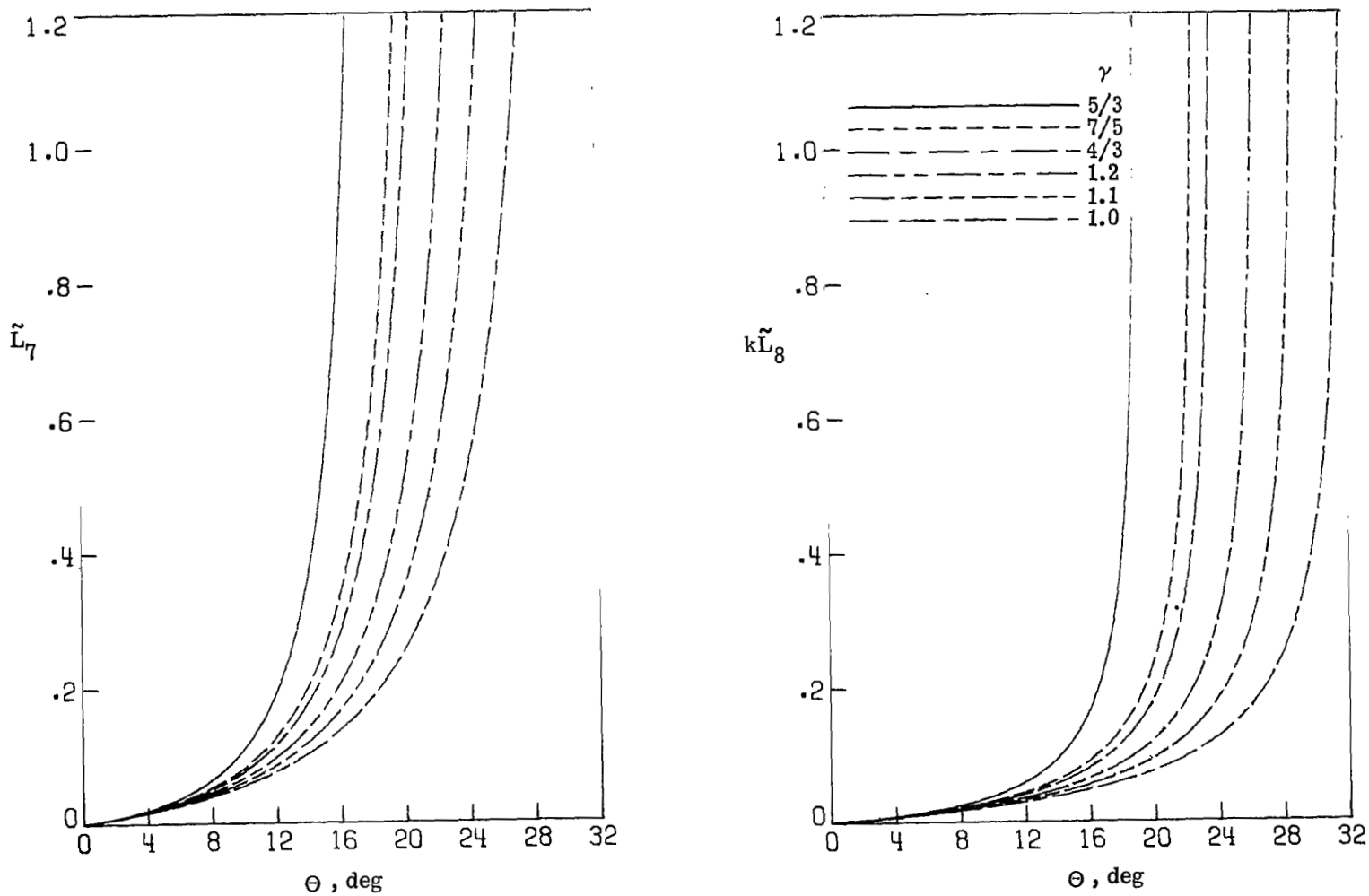

Figure 5.- Concluded.

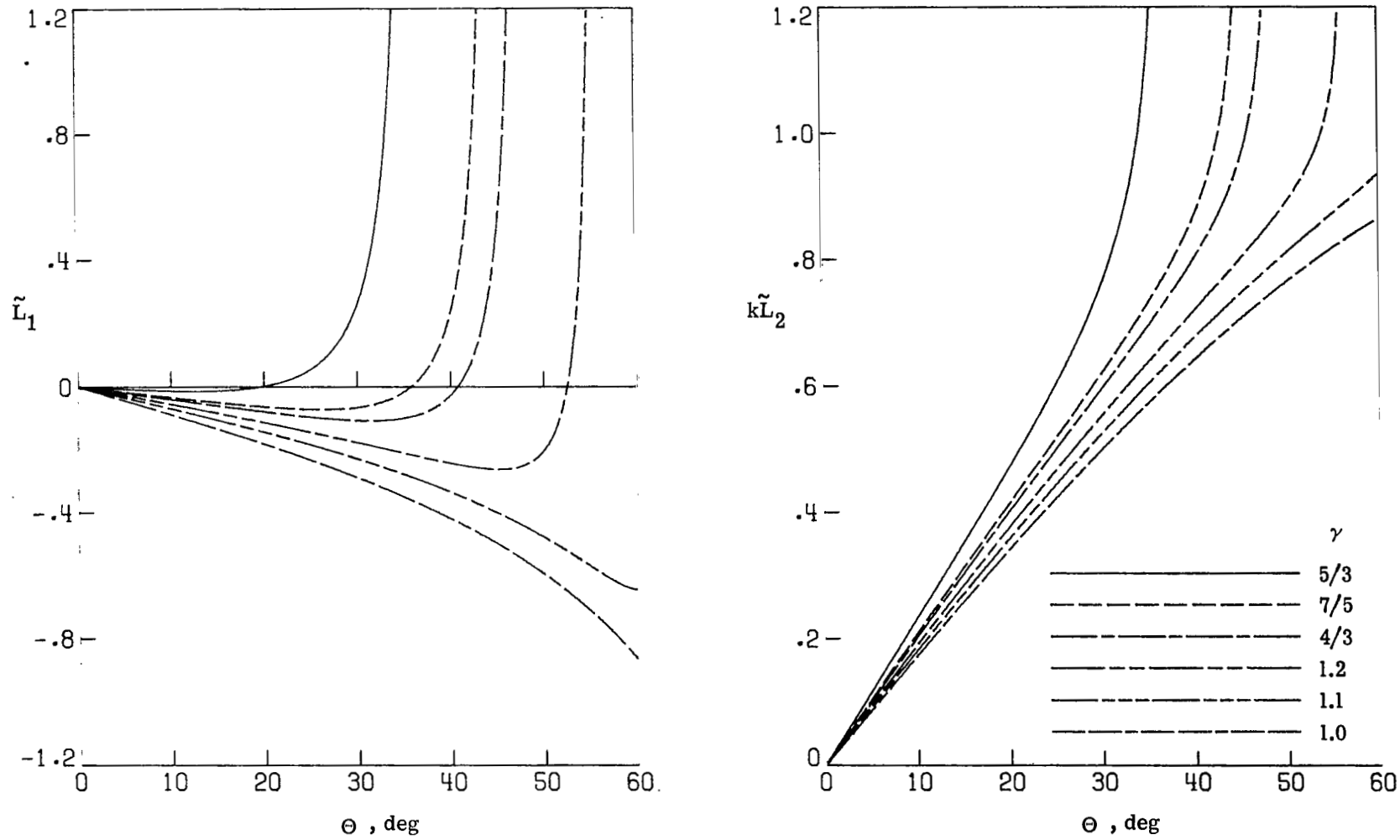

Figure 6.- Coefficients for a single surface at infinite Mach number. k = 0.

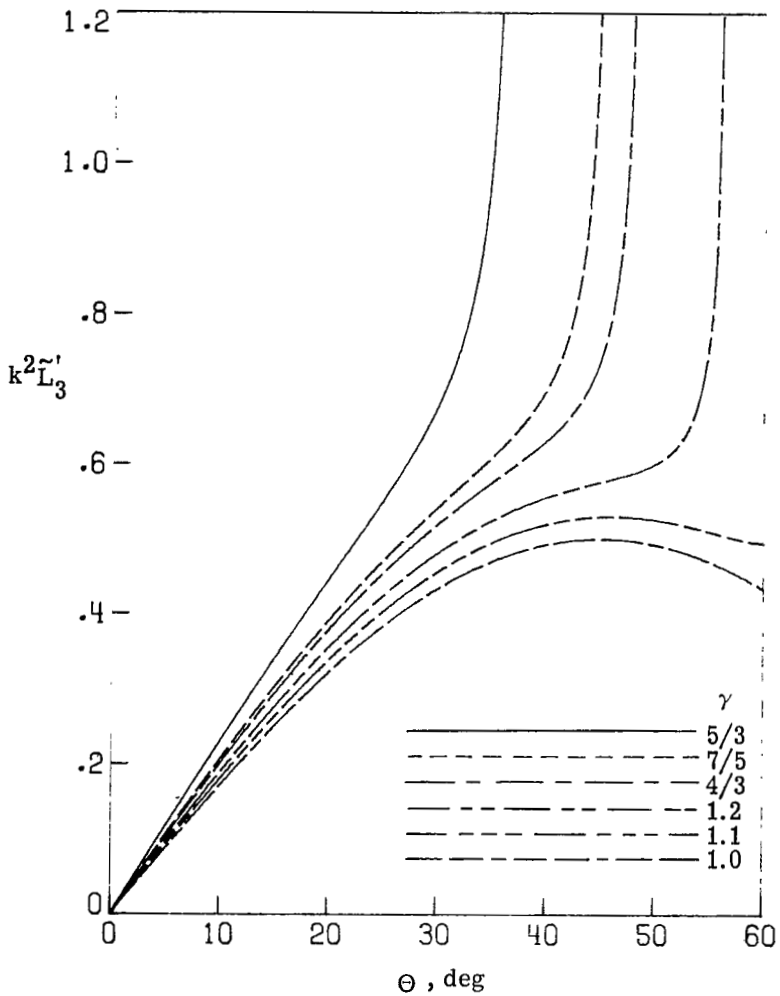

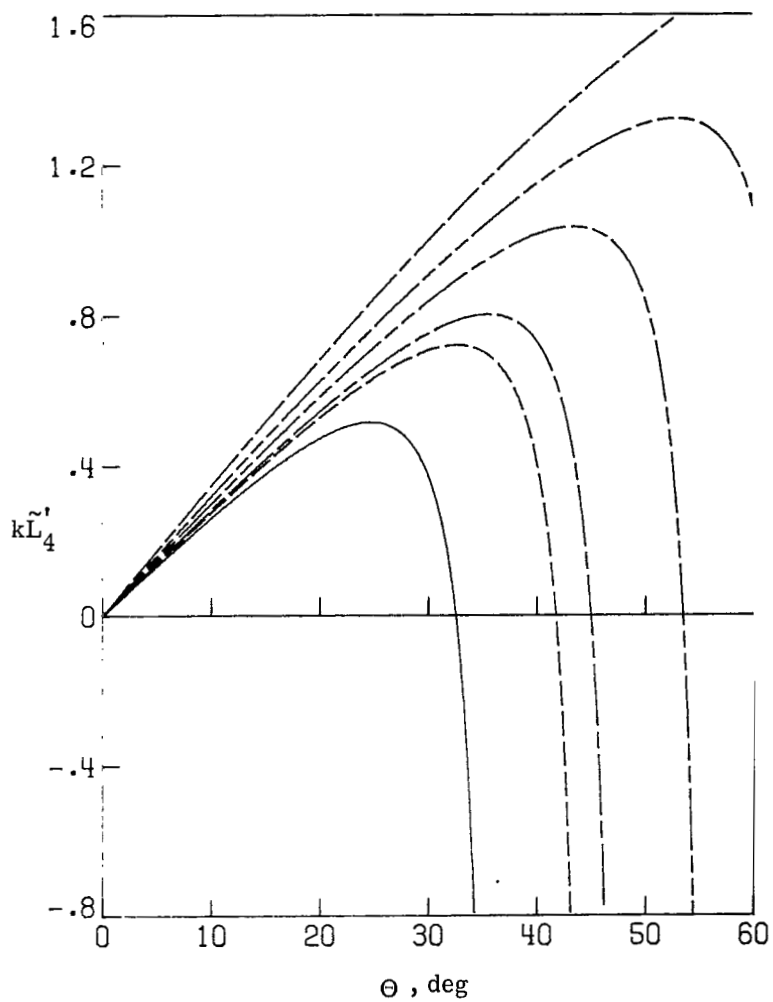

Figure 6.- Continued.

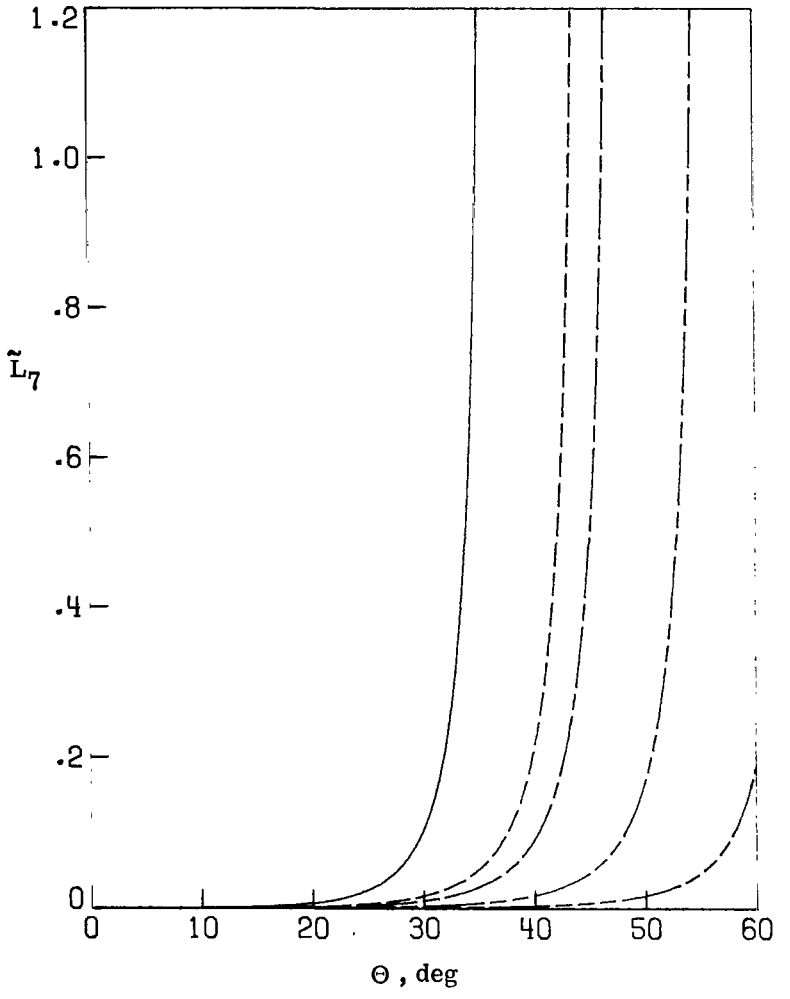

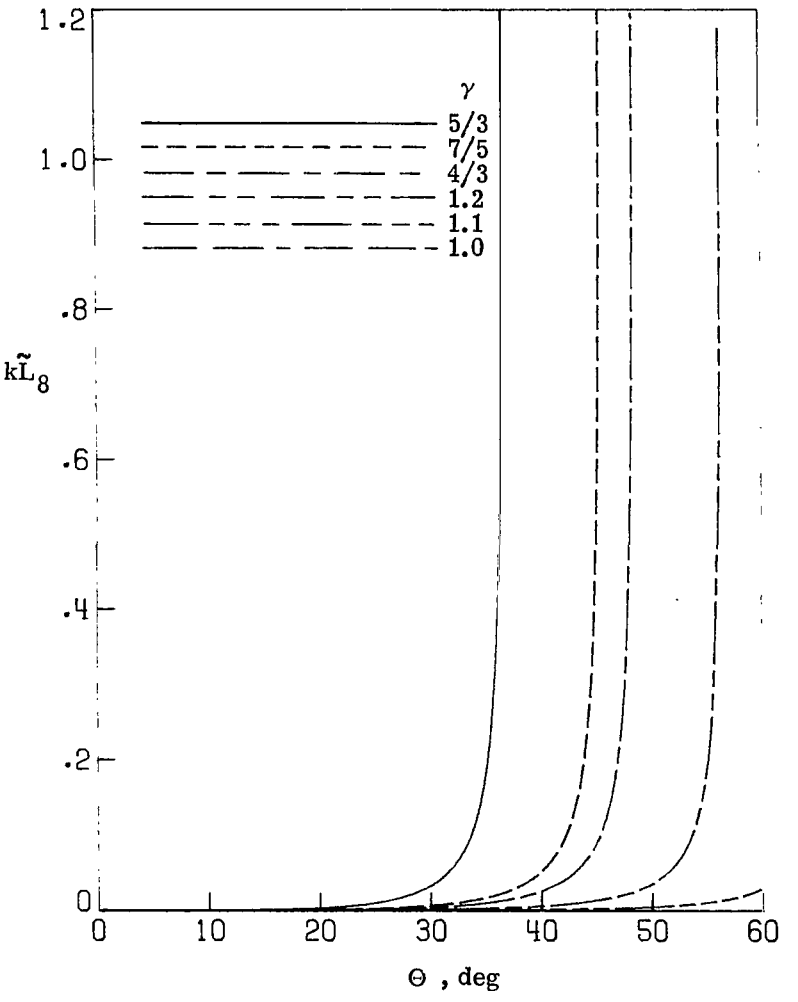

Figure 6.- Concluded.

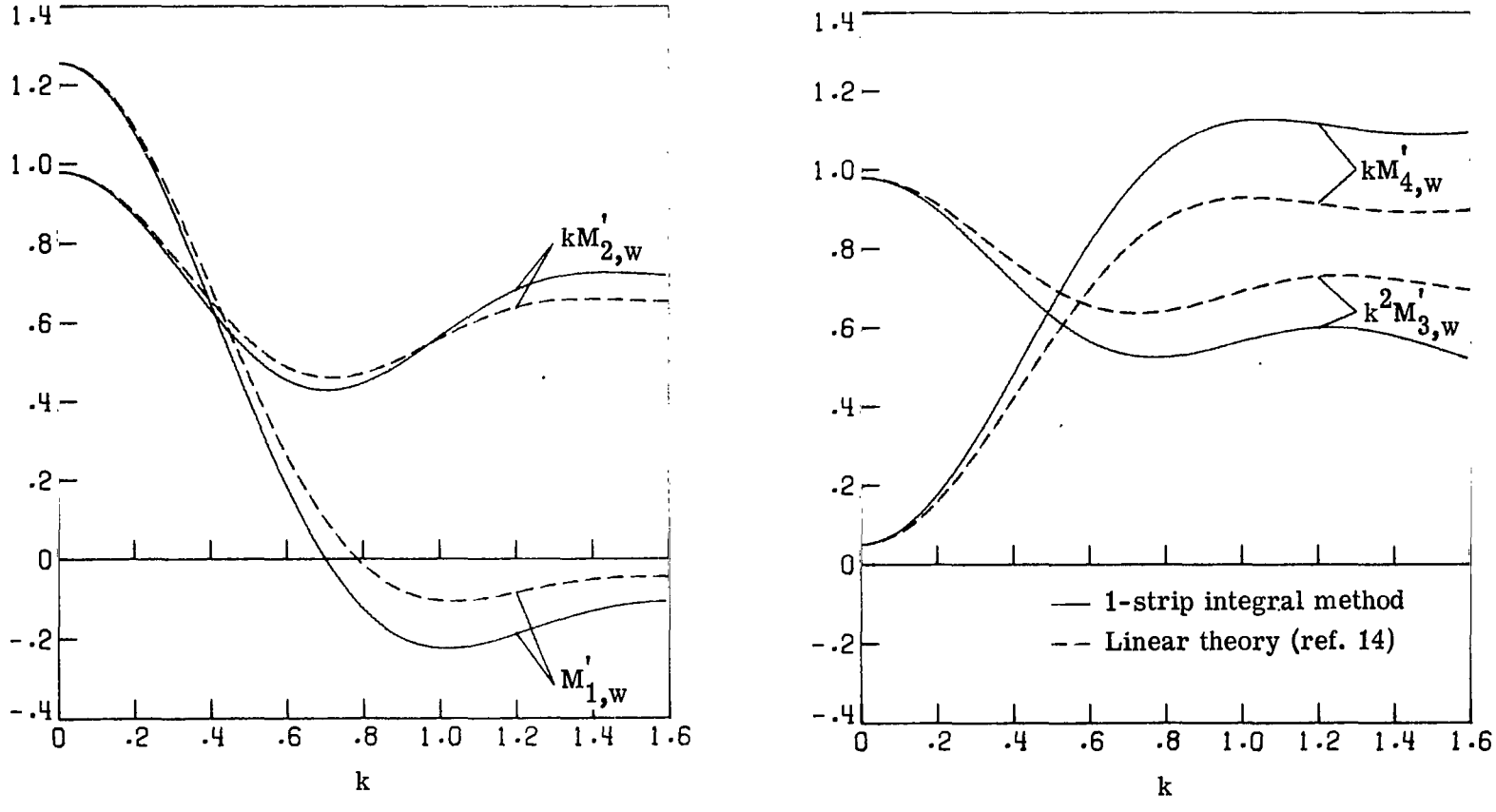

Figure 7.- Comparison of frequency effects for a wedge at a Mach number of 10/7. $\tau = 0$.

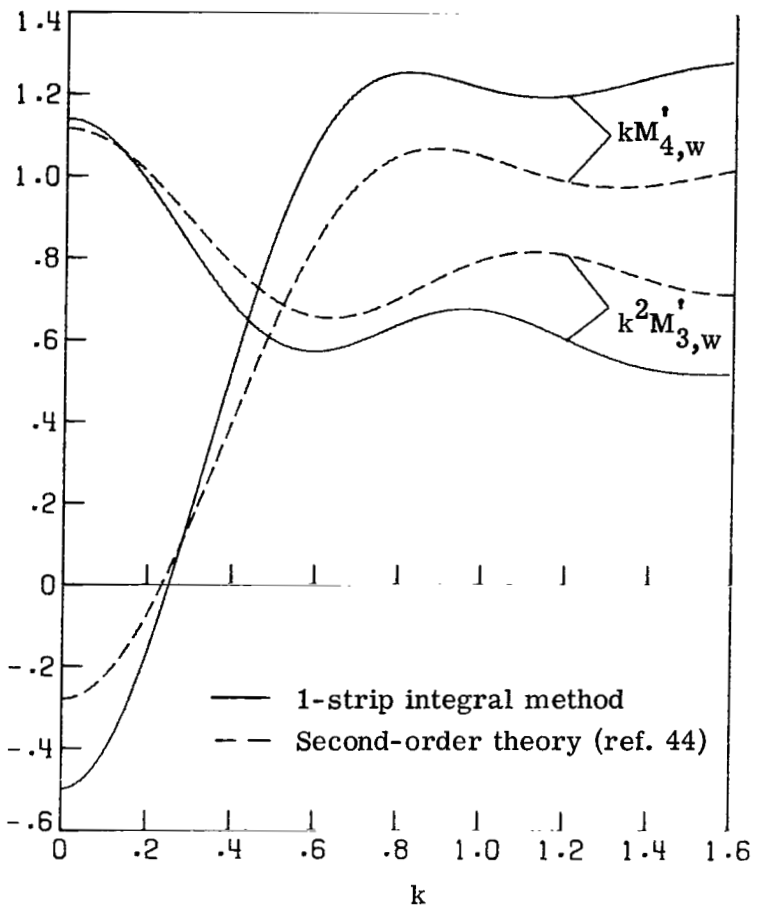

Figure 8.- Comparison of frequency effects for a wedge at a Mach number of 10/7. $\tau = 0.10$.

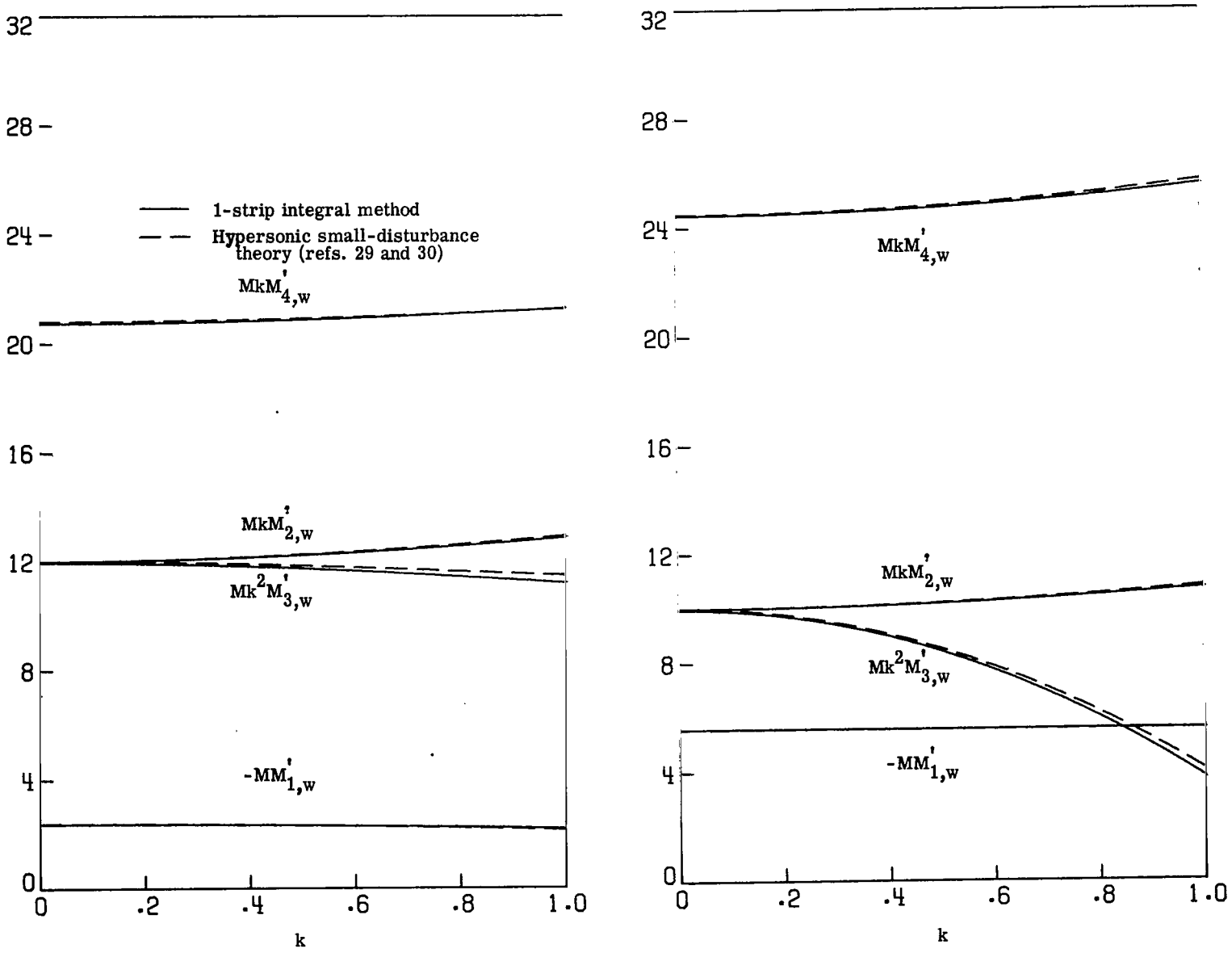

(a) $\gamma = 7/5$.

(b) $\gamma = 1.0$.

Figure 9.- Comparison of frequency effects for a 5^{o} wedge at a Mach number (M) of 57.3.

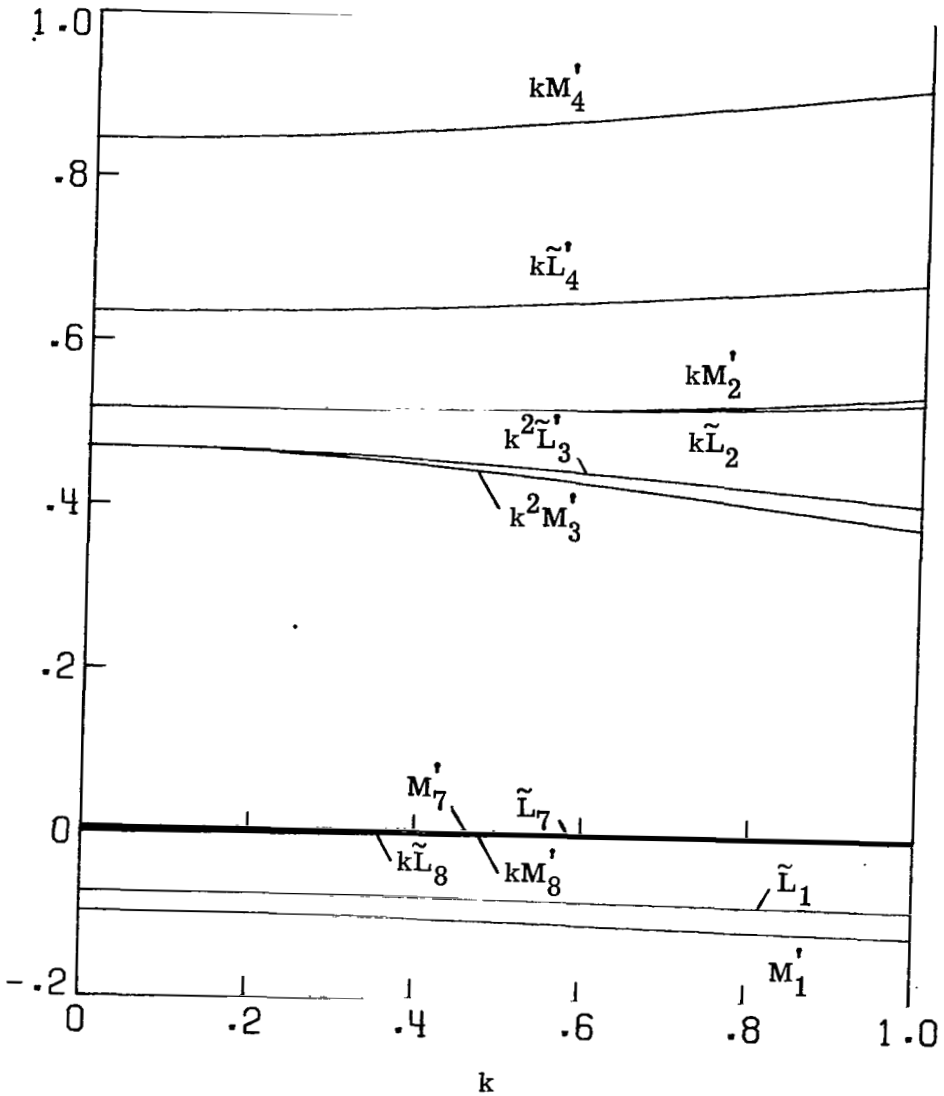

Figure 10.- Coefficients at infinite Mach number for a single surface with $\Theta = 25^{o}$. $\gamma = 7/5$.

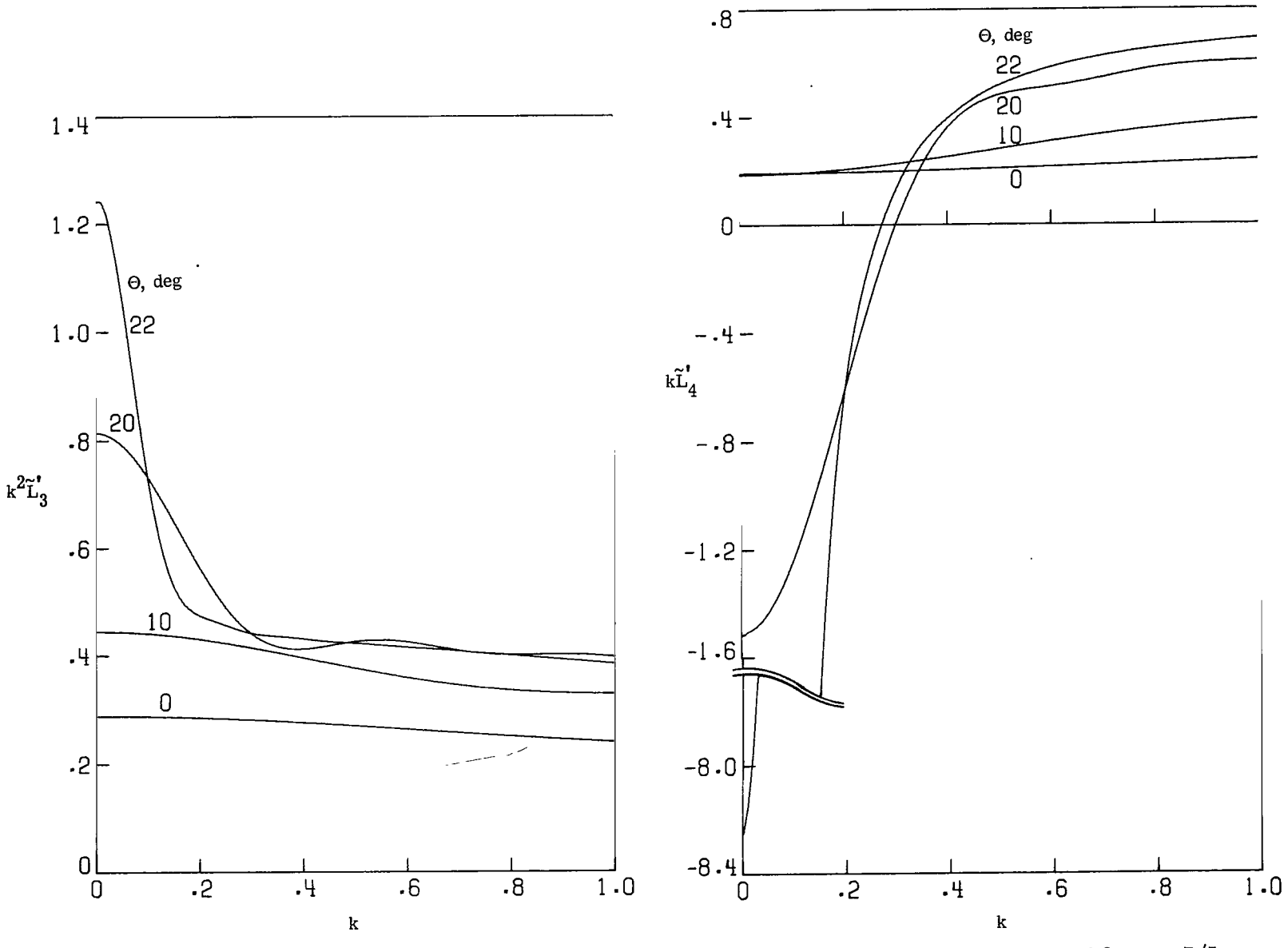

Figure 11.- Effect of k for several inclination angles of a single surface at a Mach number of 2. $\gamma = 7/5$.

NATIONAL AERONAUTICS AND SPACE ADMISTRATION
WASHINGTON, D.C. 20546

OFFICIAL BUSINESS
PENALTY FOR PRIVATE USE $300

FIRST CLASS MAIL

POSTAGE AND FEES PAID
NATIONAL AERONAUTICS AND
SPACE ADMINISTRATION

U.S.MAIL

013 001 C1 U 01 720303 S00903DS
DEPT OF THE AIR FORCE
AF WEAPONS LAB (AFSC)
TECH LIBRARY/WLOL/
ATTN: E LOU BOWMAN, CHIEF
KIRTLAND AFB NM 87117

POSTMASTER: If Undeliverable (Section 158 Postal Manual) Do Not Return

"The aeronautical and space activities of the United States shall be conducted so as to contribute . . . to the expansion of human knowledge of phenomena in the atmosphere and space. The Administration shall provide for the widest practicable and appropriate dissemination of information concerning its activities and the results thereof."

—NATIONAL AERONAUTICS AND SPACE ACT OF 1958

NASA SCIENTIFIC AND TECHNICAL PUBLICATIONS

TECHNICAL REPORTS: Scientific and technical information considered important, complete, and a lasting contribution to existing knowledge.

TECHNICAL NOTES: Information less broad in scope but nevertheless of importance as a contribution to existing knowledge.

TECHNICAL MEMORANDUMS: Information receiving limited distribution because of preliminary data, security classification, or other reasons.

CONTRACTOR REPORTS: Scientific and technical information generated under a NASA contract or grant and considered an important contribution to existing knowledge.

TECHNICAL TRANSLATIONS: Information published in a foreign language considered to merit NASA distribution in English.

SPECIAL PUBLICATIONS: Information derived from or of value to NASA activities. Publications include conference proceedings, monographs, data compilations, handbooks, sourcebooks, and special bibliographies.

TECHNOLOGY UTILIZATION PUBLICATIONS: Information on technology used by NASA that may be of particular interest in commercial and other non-aerospace applications. Publications include Tech Briefs, Technology Utilization Reports and Technology Surveys.

Details on the availability of these publications may be obtained from:

SCIENTIFIC AND TECHNICAL INFORMATION OFFICE

NATIONAL AERONAUTICS AND SPACE ADMINISTRATION

Washington, D.C. 20546